Universitat de Girona
Escola Politècnica Superior

Treball Final de Grau/Carrera

Realitzat i defensat a Odisee de Bèlgica

Estudi: Grau en Enginyeria Mecànica Pla 2009

Títol: Cabin suspension analysis and design of the Arcelor Mittal overhead cranes

Alumne: Pau Gratacós

Director/Tutor: Dr. Koen Deprez
Departament: Eng. Mecànica i de la Construcció Industrial

Convocatòria (mes/any): Juny/2015

Abstract

This work begins with a request of the company Arcelor Mittal in the Gent factory. An assessment of the comfort situation on their cabin cranes pointed out that the vibrational comfort levels are near the action levels stipulated in the European norm (ISO 2631/1) [1]. In order to improve the working comfort of the overhead crane operators the company implemented a cabin suspension that showed no actual improvement. The aim of this work is to deliver a detailed analysis of the low-frequency vibrational comfort of the overhead cabin cranes. To do so several vibration measurements have to be taken and analysed. After the analysis the company may decide to study a new suspension design knowing which vibration needs to be attenuated.

Table of contents

List of Figures

List of Tables

Symbols

Variables

$\sum$	:	combined VDV or effRMS values	
N	:	number of periods	
W_{ij}	:	frequency weighing filters	
x	:	longitudinal or driving direction	
y	:	lateral direction	
z	:	vertical direction	
T_s	:	measurement period	[s]
a_{max}	:	maximum peak acceleration	[m/s^2]
m	:	mass	[kg]
$\dot{m}$	:	mass flow	[kg/s]
$\ddot{y}$	:	acceleration of mass m	[m/s^2]
P_0	:	ambient pressure	[Pa]
P_i	:	pressure I	[Pa]
ρ_i	:	fluid density i	[kg/m^3]
A	:	effective area of air spring	[m^2]
g	:	gravitational acceleration	[m/s^2]
C_p	:	specific heat at constant pressure	[J/kgK]
T	:	temperature	[K]
V	:	volume	[m^3]
C_v	:	specific heat at constant volume	[J/kgK]
κ	:	ratio of specific heats	
S	:	surface of valve opening	[m^2]
f_B	:	natural freq. at the optimum point	[Hz]
f_s	:	natural freq. air spring alone	[Hz]
f_{sa}	:	natural freq. air spring with reservoir	[Hz]
Ω	:	ratio of natural frequencies	
k	:	stiffness	[N/m]
b	:	damping	[Ns/m]
b_c	:	critical damping	[Ns/m]
ω_n	:	natural frequency	[Hz]
ξ	:	damping ratio	
K	:	gain	

Abbreviations

LBP	:	Low Back Pain	
RMS	:	Root Mean Square	[m/s^2]
effRMS	:	Effective Root Mean Square	[m/s^2]
VDV	:	Vibration Dose Value	[$m/s^{1.75}$]
VDV8h	:	Vibration Dose Value for an 8h period	[$m/s^{1.75}$]
WBV	:	Whole-Body Vibration	
VWF	:	Vibration-induced White Finger	
PSD	:	Power Spectral Density	
FFT	:	Fast Fourier Transform	

Chapter 1

Introduction

Crane operators work with heavy equipment which results in continuous exposure to whole-body vibration (WBV). Epidemiological studies have shown a relatively strong association between occupational low back pain (LBP) and long term exposure to WBV with the risks for injury increasing as the duration and dose of WBV increases [2],[3]. Studies illustrated that the relative risk of developing LBP in heavy equipment operators compared to other work populations is more than the double [4]. The crane operators of ArcelorMittal complained about the comfort problems that they are having driving the crane and wanted an analysis or study to evaluate the vibrations at the cranes they work. The company ordered some tests and the results pointed out that the vibrational comfort levels inside the cabins were near the action levels stipulated in the European norm (ISO 2631/1)[1]. The aim of this work is to deliver a detailed analysis of the low-frequency vibrational comfort of the overhead cabin cranes. In order to do so several vibration measurements have to be taken and analysed. After the analysis is completed and discussed with the company the possibility of developing a new suspension system in order to improve the comfort levels to a less harmful level could appear.

1.1 Objective for this Project

Based on measurements performed by the company AIB-VINÇOTTE International in the cranes, showed in annex C, seems clear that the comfort situation on the overhead cranes needs to be improved. European directive [5] sets on the minimum health and safety requirements regarding the exposure of workers to risks arising from physical agents (vibration in our case). Following this directive it is problematic to operate the cranes under investigation. Knowing that during work time the operators are exposed 8 hours a day, the main objective of this project is to deliver an extensive analysis of the vibrations in and outside the cabins. Doing this it's possible to calculate the effectiveness of the current suspension and after that investigate possible solutions to reduce the whole body vibrations that the operators are exposed to.

To reduce vibration transmission to the operators, three modifications can be made in the suspensions. The first modification is a suspension system between the wheel and the chassis (primary suspension), the second one consists in floating the cabin (secondary cabin suspension), and the third one in modifying the seat design (seat suspension).

The large mass of the crane and the complex operating system make it very difficult to apply a primary suspension, making secondary cabin and seat suspensions the only available means to improve the comfort. Seat suspension systems have already been investigated and commercial systems are available and used. Concerning cabin suspension systems, the commercial solutions offered don't seem to have studies of effectiveness and are very expensive. Therefore this project will investigate possible cabin suspension and propose a solution via simulation using Matlab Simulink.

To make a new suspension concept commercially viable, it should be relatively cheap and it would be favourable if it could fit in the same space that is provided for the currently used suspension. In that way the changes to the cabin and the supporting structure are minor which makes the new suspension interchangeable with the current installed.

Chapter 2

Characteristics of vibration

The objective of this chapter is to explain the main characteristics of vibrations and the problems that they can generate to the crane operators due to long exposure.
For the correct evaluation and understanding of the effect that vibrations create on the human body several standards are available and discussed together with the European directive [5] in this chapter.

2.1 Basic comfort measurement parameters

When examining the impact of vibrations in the human body, there are several parameters that must be taken into account. Frequency, point of entry, rotation, direction, magnitude and duration are the most important factors in order to determinie how the vibration is transmitted through the body. The direction of the vibration is represented in three linear axes. These axes are for-and-aft (x axis), lateral (y axis), and vertical (z axis)[7]. There are also three rotational vectors, roll, pitch and yaw, which correspond to rotation about the x, y and z axes respectively. A graphical repesentation of this it's showed in the figure 2.1.

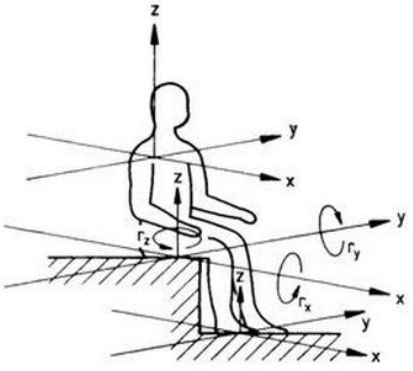

Figure 2.1 Graphical representation of the axis and rotations used in vibration analysis.

The frequency is normally expressed in cycles per second, hertz (Hz) and it represents how fast a body is vibrating. Certain vibration frequencies may have strong effects on

specific parts and systems of the human body, especially if the frequency of vibration corresponds to the resonant frequency of that part of the body. In such cases, is likely to have more pronounced effects on that area as compared to other parts of the body.

The experimental magnitude of vibration is usually represented in acceleration values (a less problematic measure than displacement and velocity). Most normatives and standards require that acceleration is expressed in (m/s2) although other units of measurement, such as ‘g’ (1g = 9.81 m/s2) are also used in specific circumstances. The absolute threshold for perception of vertical vibration for frequencies between 1 and 100 Hz is approximately 0.01 m/s2 [8]. Doubling the magnitude within this range will result in doubling of the sensation of discomfort [22].

The operator perception of comfort would also depend on their expectations (e.g., the activities they would expect to do), as well as other parameters of the vibration such as frequency and duration [1]. For example, some visual discomfort can be expected with exposure to frequencies between 60 and 90 Hz (the approximate range of resonance of the eyeballs). Representation of the magnitude of human vibration exposure is usually done with the root-mean-square RMS (m/s2). To give an estimate of the total exposure, taking duration into account, a vibration dose value (VDV) is calculated. The VDV gives an indication of the magnitude per second of duration, value that is the same severity to the measured vibration, and is expressed in m/s1.75 or in radians per second to the power of 1.75 (rad/s1.75) [1]. Calculation of the VDV vary depending on the complexity of the vibration. While a few minutes of exposure to vibration is generally thought to cause only small physiological effects (such as slight hyperventilation), the link between long-term exposure to vibration and physiological changes due to it is unclear [9].

Apart from these few factors the analysis of real vibration will be random rather than sinusoidal, and there will be changes in the frequency, direction and magnitude. This constant changes make the real analysis even more complicated. Another important factor to take into account is the point of entry of the vibration to the body. For example, if standing, vibration will enter through the feet, but if seated most vibration will enter via the lower posterior hip bone. If seated and reclining against a back rest more vibration will enter at the head and shoulders. For that reason the transmission and effects of many different types of vibration all acting on the same body at the same time can not be determined by just summing the impact of each one of them [7].

2.2 Types of Vibration Exposure

2.2.1 Introduction

Human response to vibration has been generally classified as whole-body vibration (WBV), local (segmental, hand-transmitted) vibration and motion sickness [22]. Another type of exposure which will not be discussed in this work is impact vibration, which refers to exposure to a single impact or shock (e.g., hammering a nail).

The distinction between whole-body vibration and other more specific forms of vibration is not precise. All types of exposure will result in transmission of vibration throughout the whole body and whole-body exposure commonly has localised components like local vibration of the head, hand, arm or feet.

The frequency-dependent effects of vibration on humans are summarised in Figure 2.2.

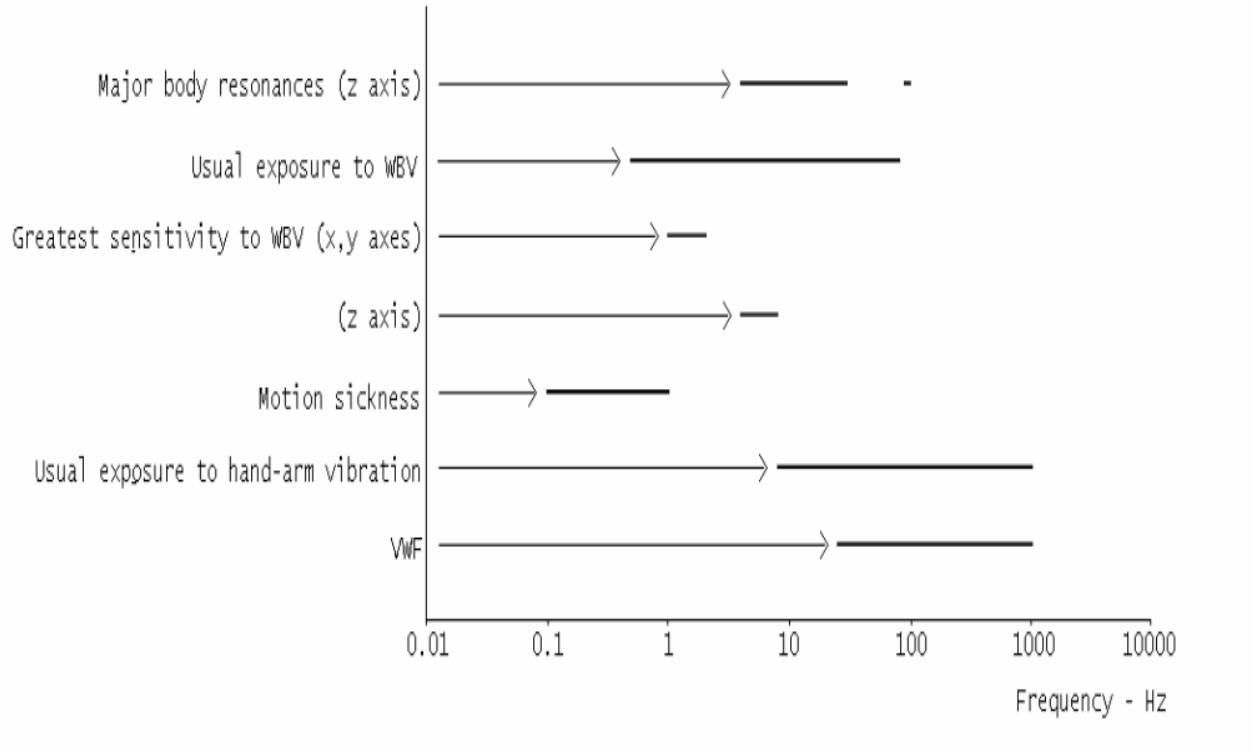

Figure 2.2 Frequency-dependent effects of vibration on humans [22].

The Figure 2.2 show that the most problematic frequencies in terms of sensitivity to WBV are between 1 and 10 Hz. That is the reason because the project focus especially in the low-frequencies that affect the cabins.

2.2.2 Whole-body Vibration (WBV)

Whole-body exposure to vibration appears when a body is supported on a vibrating surface. In most cases this occurs when one is sitting on a vibrating seat, standing on a vibrating floor, or lying on a vibrating bed [22]. Usually WBV is experienced in transport and it usually involves vibration frequencies between 0.5 to 80 Hz [7]. WBV does not affect one specific target organ, and has been associated with a variety of health problems like backaches, gastrointestinal, reproductive system, visual and vestibular disorders [10],[11],[12]. There is also evidence of intervertebral disc problems and degeneration of spinal vertebrae [13],[14]. The effects of whole-body vibrations to the human body will be discussed later in this project.

2.2.3 Local vibration

Local vibration has been used to refer to exposure when vibration is transmitted from a vibrating surface to part of the body. This exposure is also referred to as hand-arm, or hand-transmitted vibration, as it most commonly occurs with the use of vibrating tools, which are often hand-held. Most tools vibrate in the range of 8 to 1000 Hz [7]. Local vibration has been associated with circulatory disorders, bone and joint disorders, neurological disorders, muscle disorders and other general disorders (e.g., central nervous system) [7].

The most common health problem associated with exposure to vibration by the use of hand tools is the vascular disorder most commonly known as vibration-induced white finger (VWF), which appears due to damage of the small blood vessels of the fingers. This only happen after long-term exposure to hand-transmitted vibration (it can take 4-10 years before symptoms begin), and is characterised by blanching of fingertips (progressing to whole fingers), and reducing the sensitivity, followed by a sudden return of blood (red flush) with intense pain [22].

Bone and joint disorders (e.g., osteoarthritis, degeneration or deformity of bones of the hands, decalcification, cysts, and vacuoles) are associated most frequently with percussive vibration between approximately 10 and 50 Hz [7].

2.2.4 Motion Sickness

Motion sickness results from exposure to frequencies below 1 Hz, more particularly those below 0.5 Hz [7]. Symptoms are many and varied, but may include vomiting, nausea, sweating, spatial unease, drowsiness, and dizziness [22]. While motion sickness is most common in children, and many fail to show signs of susceptibility in adulthood, it has been demonstrated that everyone may be made sick if the appropriate stimulus is used [7]. Symptoms are most frequently observed in moving vehicles but there are a number of other environments where motion sickness may be initiated (e.g., fairground devices, simulators, microfiche readers, swimming [7].

2.3 An Overview of the effects of exposure to WBV

2.3.1 Introduction

In this project the main effects of the exposure to WBV are explained as this is the type of vibration that the operators are suffering the most. So far several epidemiologic studies tried to find evidence of a clear exposure-response relationship between whole-body vibration and low back pain. Complications arise because vibration exposures are often associated with jobs with other undesirable features: Tractor drivers often twist their spines to look behind the tractor, tractor and truck drivers often lift heavy loads and jump down from high cabs, bus drivers sit for long periods... This makes it difficult to point WBV as the main cause for low back pain. Nonetheless many researchers [7],[11],[15],[16] are convinced of the increased risk that exposure to WBV poses on the occurrence of LBP. The influence of a small change in posture can be large (and this influence is greater at higher frequencies), as minor changes in muscle tension and position can affect where vibration enters the body, and how vibration moves throughout the body [22]. Poor posture at the head and lower back, for example, might result in increased transmission of vibration up the head and spine [7]. In general, increased body size is associated with reduced z-axis seat to head transmission of vibration for most frequencies between 1 and 100 Hz [7]. Transmission of vibration may also vary with age and gender. For example, susceptibility to motion sickness is higher for females, and usually decreases with age

(for both males and females). With regard to comfort, females are more sensitive to certain frequencies of vibration than males [7]. Experience of vibration can result in habituation, and also better prepare the individual to respond (e.g., through changes in posture), thus reducing the impact of vibration. Experience, along with personality and attitude are also likely to influence expectations of vibration (how it will feel, how much it will interfere with activities etc.) that in turn will influence how it is perceived, and how the body changes in response to it. Thus, response to vibration exposure is highly individual, such that it is difficult to generalise very specific effects from person to person. Likewise, extrinsic variables, including the characteristics of the vibration, as well as other stressors such as noise and temperature, and seat dynamics, mean that generalisation from exposure in one environment to another is problematic [22].

2.3.2 Physiological and Pathological Changes

Vibration can cause changes to the body in an extensive number of ways. For example, hyperventilation, which is caused by the passive movement of vibration through the abdominal wall, is basically a result the mechanical effects of vibration (i.e., exposure to vibration causes various internal organs to vibrate) [22]. An increase in heart rate is also observed at the beginning of exposure, but is believed to be a stress response [17]. Higher oxygen consumption is also associated with exposure to WBV. The level of influence such changes will have on functioning is dependent on the individual, and also on the task at hand. For example, moderate to high magnitudes of vertical vibration in the range from about 2 to 20 Hz produce a cardiovascular response similar to that normally occurring during moderate exercise [7]. However, if the individual exposed to vibration is completing a very stressful task that results in a high stress response (i.e., high heart rate, oxygen consumption etc.), even a small cardiac change as a result of vibration exposure could potentially have large impact upon health, safety and performance [22].

Whilst various studies have reported small biochemical changes (blood count, endocrines, uric acid, enzyme levels, gastric secretions etc.) following exposure to vibration, generally they have not been significant, and levels observed were still within the normal physiological range [12]. Such results suggest that in most cases of exposure to vibration these changes are unlikely to have an effect on functioning.

Disorders of the back (e.g., back pain, displacement of intervertebral discs, degeneration of spinal vertebrae, osteoarthritis) have commonly been associated with exposure to vibration. Severity and incidence is variable, and in some cases onset of mild to severe back pain can occur after only short periods of exposure to vibration [22]. There is some disagreement as to the level of influence that other factors, particularly posture, may have on development of such problems, but most researchers acknowledge that posture is likely to be a large contributor to much of the back pain reported by those who work in vibrating environments [18].

Other problems associated with WBV include abdominal pain, digestive disorders, urinary frequency, peripheral vein damage, female reproductive system damage, prostatitis and haemorrhoids to name a few [22]. Balance and visual disorders, headaches and sleeplessness have also been observed [7]. Most of these conditions have been observed following long-term exposure to vibration for long durations. Some, such as sleeplessness, are most frequently associated with exposure to hand-arm vibration [7].

Unfortunately, there is little research on the likelihood of developing these problems as a result of less frequent exposures of shorter durations. Most researches tends to examine the effects of a few minutes or seconds of exposure (i.e., laboratory studies or sudden impacts), or several years of exposure to vibration for long durations (i.e., epidemiological studies). While the likelihood of development of most disorders tends to increase with increased magnitude and duration of exposure to vibration, the impact of vibration on those exposed for durations that fall in between the extreme short-term and long-term is not well known [22].

Several conditions have been attributed with the exposure to vibration within specific ranges of frequencies. The influence of frequency on the body is accounted for in a very general sense by frequency weightings, where frequencies of greater influence (i.e., requiring lower magnitudes to have an effect) are given higher weighting values. Human sensitivity to WBV is highest around 4-8 Hz in the z direction, and 1-2 Hz in the x and y directions [19]. At very low frequencies (i.e., less than 2 Hz) of vertical vibration, most body parts move up and down in unison. The sensation tends to be one of being pushed up and then floating down. Activities involving use of the hands may be affected by disturbances to free movement of the hands. Below 1 Hz (usually below 0.5Hz) motion sickness may occur. Low frequency horizontal vibration tends to cause the body to sway (although this may be resisted through muscular action or seating support) and it

becomes difficult to stabilize the upper body, and quite uncomfortable. With increasing frequency, horizontal vibration is less well transmitted to the upper body [7].

Pains in the chest and abdomen have been observed with exposure to vibration ranging from 4 to 10 Hz, while backaches commonly occur at 8-12 Hz. Headaches, eyestrain, and irritations in the intestines and bladder occur between 10-20 Hz [20]. Spinal and upper torso problems occur at 10-12 Hz; head and neck occurs at around 30 Hz; and, the eyeballs are at 60-90 Hz [8]. With regard to high magnitude, high frequency vibration, respiratory problems and giddiness have been observed at 60 and 73 Hz, and mild nausea, giddiness, subcostal discomfort, cutaneous flushing and tingling have been observed at around 100 Hz [21], but it should be noted that these vibration levels were high magnitude, induced by high intensity noise. Although substantial fatigue was reported following exposure to high magnitude vibration (in excess of 10 m/s2) for durations of at least 2 minutes [21], there is little other information concerned with the association between fatigue and vibration exposure [7].

2.3.3 Performance Effects

Vibration has been observed to have an impact on performance of various tasks, involving vision, motor activity, and information processing [22]. Performance is worse when there are various frequencies of vibration occurring at the same time, and better when vibration is random (although more uncomfortable) [17]. This effect may be due to the direct effects of vibration on input and output processes (e.g., vision, hand movements), or indirect effects, through other changes such as motivation, mood, and arousal. In cases where vibration results in arousal, and better performance of particular tasks, it is also important to consider that this may occur at the expense of performance on other tasks, and result in earlier fatigue [22]. It has also been noted that different types of vibration may lead to use of different strategies (for example a task may be completed with fewer errors, but at a slower rate) [7].

One of the main performance issues due to vibration is the negative effect that it has on vision. The effects of vibration on vision depend on the extent to which the vibration is transmitted to the eye. Below frequencies of about 10 Hz, the ‘vestibulo-ocular reflex’ will compensate for pitch motions of the head, thus maintaining the line of site [7]. Such head movements will have little impact on vision, unless information is presented on a head-

mounted display. Visual performance is most impaired in the range of 10-25 Hz [9]. The threshold for visual detection that an object is vibrating is very low for low frequencies and high for high frequencies. Above this threshold there will be perceptible blur due to the movement of images over the retina [7].
Completion of tracking tasks has been used in various studies as an index of motor performance. It has been found that vibration between 4 and 20 Hz (at accelerations exceeding 0.20g) has a detrimental effect on such activity, and that there is still an effect up to 30 minutes after exposure to vibration has ceased [9]. Exposure time does not appear to affect performance up until around 3 hours of exposure, such that a longer exposure to vibration does not result in a higher error rate [9].

2.4 Regulation of vibration and European directive

In order to regulate the working vibration environment there are three human response to vibration standards of main interest. ISO 2631-1(1974) [6], ISO 2631-1(1997) [1] and BS6841(1987) [23]. This standards provide several steps to follow for a proper analysis and also give limit numbers to classify vibration severity called comfort values. Those values are used in the European directive 2002/44/EC [5] for determining the maximum values that the operators can be submitted to. This work follows the standards and directives in how to do a proper analysis and give standardized results.
The values to present are the effective or weighted RMS (effRMS) and the vibration dose value (VDV). These values are calculated for every axis and rotation based on filtered acceleration data that has been taken using accelerometers in the place to analyse.
In numerous cases the RMS of the frequency weighted accelerations is a useful indicator of the severity of the vibrations. But if the vibrations are non-stationary or include a large number of shocks, the VDV is a better indicator [7]. Determining factor in this is the crest factor a factor that shows us if the vibrations are stationary or not. If the crest factor it's lower than 7 then we can consider that the vibrations are stationary [7].
In this work we will also provide the VDV value for 8h of work, another parameter very useful in our analysis since the operators work on an 8h daily basis.
As mentioned before in the European Directive 2002/44/EC [5], certain limit and action values are given for the daily exposure to vibrations. Every member state has the option

to maintain these minimum requirements or adopt them to a more favourable values for the protection of workers.

The daily exposure limit value is set to an effRMS of 1.15m/s^2 or a VDV of 21 m/$s^{1.75}$ over an eight-hour reference period and the daily action value is for that same eight-hour period put at an effRMS of 0.5m/s^2 or a VDV of 9.1 m/$s^{1.75}$ [5].

This values can not be violated and once they are, the company has to implement a technical program to reduce the exposure to vibrations.

2.5 Conclusion

After the review of the problems that the vibration can cause to the body seems clear that the operators of the cranes may need some changes. The two only ways to solve the problem are either reducing the exposure time or reduce the magnitude of the vibration (particularly in the most damaging frequencies). In this case reducing the exposure time would be desirable but it is not possible. As a result of that a modification of the cabin suspension should be designed.

The vibration that the operators suffer doesn't seem much for an external person that operates the machine for one day because the vibration is easy to handle for a short period of time. The real problem starts when they face the vibration of the crane every day during years, they suffer the consequences and the problems increment during time being low back pain one of the most common problems.

The European directive has their maximum comfort values for trying to avoid or at least reduce this problems. The parameters are reviewed periodically and certainly the values will be lower and lower until, one day, they reach a point where these vibration problems will not exist anymore thanks to the constant development of suspension systems.

Chapter 3

Comfort improving suspension systems

This chapter discus the most common used suspension systems to solve vibration problems.

Vibration transmission can be reduced by three modifications in the suspensions. The first modification is using a suspension system between the wheel and the chassis (primary suspension), the second one consists in floating the cabin (secondary cabin suspension), and the third one in modifying the seat design (seat suspension).

As said before the large mass of the crane and the complex operating system make it very difficult to apply a primary suspension so in this chapter we will only focus on secondary cabin suspensions and seat suspension.

Finally, this chapter discus which system could fit better the specifications in the crane of the study without knowing yet the vibrational behaviour of the system.

3.1 Cabin suspension systems

3.1.1 Introduction

A cabin suspension is the system of springs, shock absorbers and linkages that connects the body of the crane with the cabin and allows relative motion between them. The design of a cabin suspension system can be done with many different methods. This apparat describes and illustrates the basic characteristics of some elements that combined with the design of the machine structure can assemble a proper suspension.

3.1.2 Coilovers

A coilover is a very common automobile suspension device. "Coilover" is short for "coil spring over shock". It consists of a shock absorber (hydraulical damper) with a coil spring encircling it. The shock absorber and spring are assembled as a unit prior to installation, and are replaced as a unit when the shock absorber has leaked. This provides for optimal damping without torsional loads. Stiffness can be changed by switching the spring for one with a different spring rate.
In most shock absorbers, energy is converted to heat inside the viscous fluid which make the fluid to heat up. In the actual crane suspension there are four hydraulical dampers installed. This type of suspension isn't really frequent in heavy machines because it doesn't perform well working in high frequencies. In such conditions the hydraulic cylinder (damper) works as a solid because the fluid doesn't have time to adapt to the fast changes and can't dissipate the vibrations.

There are several types of coilovers that are not discussed here because they are mainly used in car suspensions, see Figure 3.1.

Figure 3.1 Different types of coilovers from left to right: Coilover sleeves, Non shock adjustable coilovers, Shock adjustable coilovers and Shock adjustable coilovers with camber kit.

3.1.3 Air springs

The air spring damper is a type of suspension that is powered by an air pump or compressor. The air springs are the normally used in truck and tractor cab suspensions as they work well in heavy machines [24].
Air springs used for cabin suspensions are arranged as four-corner suspension between the driver's cab and the chassis frame, the first crane of the study has this system installed. Air springs are very versatile as a manufacturer can use a uniform component regardless of customer variant and equipment preferences.

There are two main different air springs in the market, see figure 3.2.

- Rolling Lobe air springs:

  Rolling lobe air springs have a low natural frequency and a high degree of lateral flexibility. They also give high spring deflection or lift by means of length change without the need to change the diameter. This advantage means that vehicle bodies can be raised or lowered with the aid of air springs used as axle springs, without additional equipment being required [26].

- Convoluted air springs:

  Convoluted air springs are characterised by a favourable height to spring deflection ratio (with this type of air spring a relatively high spring deflection can be achieved with the smallest amount of overall height) [26].

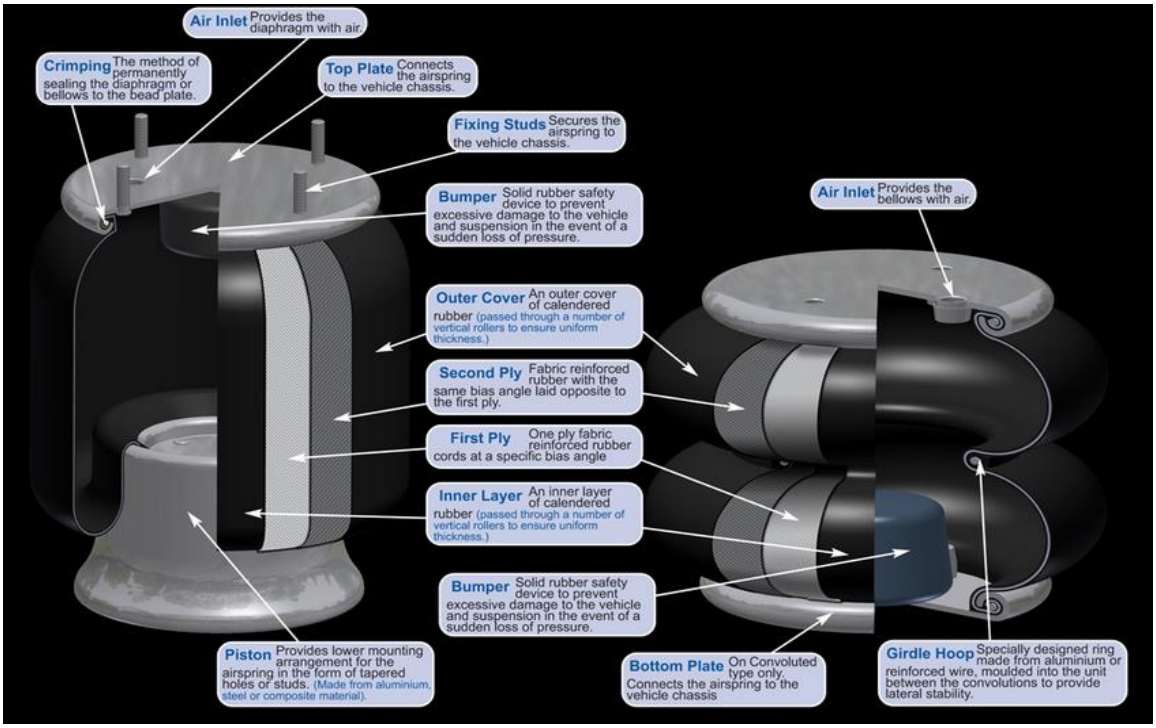

Figure 3.2 Parts of the rolling lobe air spring in the left and convoluted air spring in the right [26].

The common problems with this suspension system are the air struts, usually caused by wet rot, moisture or air fitting failure which occurs when the system is first fitted or very rarely in use. This problem makes the air system burn out the compressor which try to maintain the correct air pressure in the leaking system [25].
A recently new variation of this system is the connection of an air spring with an external air reservoir using a throttle valve to regulate the air that can flow from one recipient to the other. This system isolates better the cabin because it smooth the transaction of air that comes in an out the air spring and it also lowers the natural frequency of the system [24].

3.1.4 Leaf springs

A leaf spring is a simple form of spring which takes the form of a slender arc-shaped length of spring steel of rectangular cross-section. For very heavy vehicles, a leaf spring can be made from several leaves stacked on top of each other in several layers, often with progressively shorter leaves. Leaf springs can serve locating and to some extent damping as well as springing functions. A leaf spring can either be attached directly to the frame at both ends or attached directly at one end, usually the front, with the other end attached through a shackle, a short swinging arm. Different types of leaf springs can be seen at figure 3.3. The second crane of the study has a leaf spring system installed. This springs can not be used with a low spring constant as their natural structure makes it impossible.

Figure 3.3 Different types of leaf springs designs.

3.1.5 Hydro-pneumatic suspensions

This system was created by the company Citroen and is a very effective suspension system but is complex and needs space to be implemented. It works like a damper but in a more sophisticated way. Nitrogen is used as the trapped gas to be compressed, since it is unlikely to cause corrosion. A nitrogen reservoir with variable volume yields a spring with non-linear force-deflection characteristics. The actuation of the nitrogen spring reservoir is performed through an incompressible hydraulic fluid inside a suspension cylinder. The nitrogen gas within the suspension sphere is separated from the hydraulic oil through a rubber membrane. Spheres consist of a hollow metal ball, open to the bottom, with a flexible desmopan rubber membrane, fixed at the 'equator' inside, separating top and bottom. The top is filled with nitrogen at high pressure, up to 75 bar, the bottom connects to the hydraulic fluid circuit. A high pressure pump, pressurizes the hydraulic fluid and an accumulator sphere maintains a reserve of hydraulic power. This part of the circuit is at between 150 and 180 bars [37].

Pressure flows from the hydraulic circuit to the suspension cylinders, pressurizing the bottom part of the spheres and suspension cylinders. Suspension works by means of a piston forcing the incompressible hydraulic fluid into the sphere, compacting the nitrogen in the upper part of the sphere; damping is provided by a two-way 'leaf valve' in the opening of the sphere. The incompressible hydraulic fluid has to squeeze back and forth through this valve which causes resistance and controls the suspension movements. It is the simplest damper and one of the most efficient. In figure 3.4 it’s shown an overview of the system [37].

Hydro-pneumatic suspensions have a number of natural advantages over steel springs, generally recognized in the automobile industry. The nitrogen gas (air) as spring medium is approximately six times more flexible than conventional steel, so self-levelling is incorporated to allow the vehicle to cope with the extraordinary suppleness provided. The only problems of this systems are the design complexity and the need of space [37].

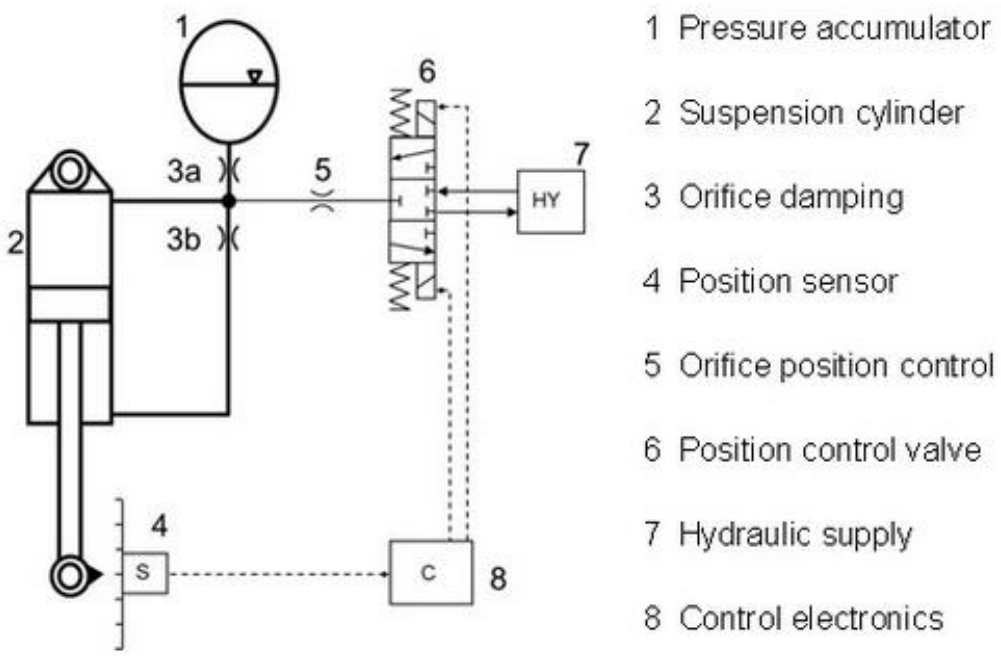

Figure 3.4 General overview of the hydro-pneumatic suspension system [37].

3.2 Seat suspensions systems

3.2.1 Introduction

Most exposures to vibration occur when individuals are seated, as happens in the crane operators, for that reason it is important to consider how the properties of the seat design might influence the transmission of the vibration. A good designed seat can reduce the exposure to WBV. For example, at low frequencies a backrest can help to stabilize the upper body and reduce the effects of motion. In contrast, at high frequencies the backrest is the major cause of transmission to the upper body, and can greatly increase the effects of fore-and-aft vibration [7].

For that reason the complexity of the design comes when we have a mix of low frequency vibration and high vibration environment.

3.2.2 Conventional seats:

The conventional seat is the one used basically in cars, it has cushions made out of polyurethane foam reinforced with metal or rubber springs. This seats reduce the vertical transmission of vibrations at frequencies higher than 6 Hz, studies show resonances in the region of 4 Hz with an amplification factor up to two or more. [24] The backrest and the seat pan exhibit three resonance frequencies below 60 Hz in the for-aft direction and a very poor attenuation level at the sat pan in this directions [27]. This problem could be solved changing the foam properties but until now most of the seat designs in the automotive industry are based on experience form previous designs without the benefit of a clear understanding of the properties of the foams sand the seat-occupant interaction [24].

3.2.3 Suspended seats:

The suspended seat is similar to the conventional one but it incorporates a suspension mechanism that linkages the ground and the seat. This type of seat is used as driver seat on busses, trucks, tractors and cranes. This seat system uses a kind of scissor system which is low in production and highly packable. It also includes a spring and a damper to give a substantially lower resonance frequency which also improves the seat isolation characteristics [28]. One of this seats is incorporated in the crane and it is a commercial model with a good studied design so in this project it is not intended to improve it. An example of this seat can be seen at figure 3.5.

Figure 3.5 Commercial suspended seat.

3.3 Conclusion

This chapter has given an overview of the most common used elements for cabin suspension and seat suspensions. In the cranes of our study there are two different systems installed and they do not isolate properly the cabin. The seat suspension implemented in the cranes it is quite good so our main occupation is to choose a system that will improve the comfort of the operators by using a suspension between the structure and the cabin.

To make a new suspension concept commercially viable, it should be relatively cheap and it could be favourable if it would fit in the same space that is provided for the currently used suspension. In that way the changes to the cabin and the supporting structure are minor which makes the new suspension interchangeable with the current solution.

Given the characteristics of the crane the first solution that comes to mind is trying to install an air spring with an auxiliary reservoir as it would fit well in the existent place, it's not really expensive and it's given good results in other similar situations [24]. This could be implemented to the first crane which has already air springs installed in a very simple way.

The next step in the project is the assessment of the vibration comfort inside and outside the cabin in order to study the actual values of vibration and isolation and determinate if the air spring with an auxiliary reservoir could be a good solution.

Chapter 4

Assessment of the vibrational comfort

To be able to have an overall analysis of the vibrations on the overhead crane it is important to analyse the present situation. The analysis has been performed on two different cranes in different working conditions. The first section describes the cranes and how they work. The second section gives an explanation of how the analysis in the field is done and which tools are used. In the third it is explained how the data is filtered and analysed using Matlab. Finally the results and interpretations of the analysis are performed.

4.1 Introduction

The two cranes studied in this project are overhead cranes used in the Gent factory of ArcelorMittal, one of them is shown in figure 4.1. This cranes can load up to 105 tons, the operator sits in a cabin 12 m high from the ground and the length between the supports of the crane is of 14 m. The cranes can move forward and backwards 60 m approximately in the rails installed in the factory, picture of the rails in figure 4.2. The cabin is rectangular and suspended, with glass on the frontal, lateral and even in a part of the ground for allowing better visibility to the operators. A picture of the first cabin studied can be seen at figure 4.3 and a technical drawing of it at figure 4.4.

The main purpose of this overhead crane is to move the iron blocks that come out from the oven in a rectangular shape, to the next step of the production process using the massive gripper that has incorporated, see figure 4.5. This cranes can move forward and laterally simultaneously, movement that the cabin and the grippers do together. Finally the grippers can move up and down for picking up the blocks, direction in which the cabin does not move.

The cabins have installed a suspension system with four hydraulic dampers. One of the hydraulic dampers is shown in the figure 4.6. In the first crane there is also installed an

air spring damping system. In the second crane there are also the four hydraulic dampers and instead of air springs there are two leaf springs installed. One of the leaf spring suspension was broken and the cabin was fixed to the structure in the days of testing. This resulted in a bigger stiffness to the system which only used one leaf spring to isolate the cabin.

Figure 4.1 One of the overhead cranes analysed in the project.

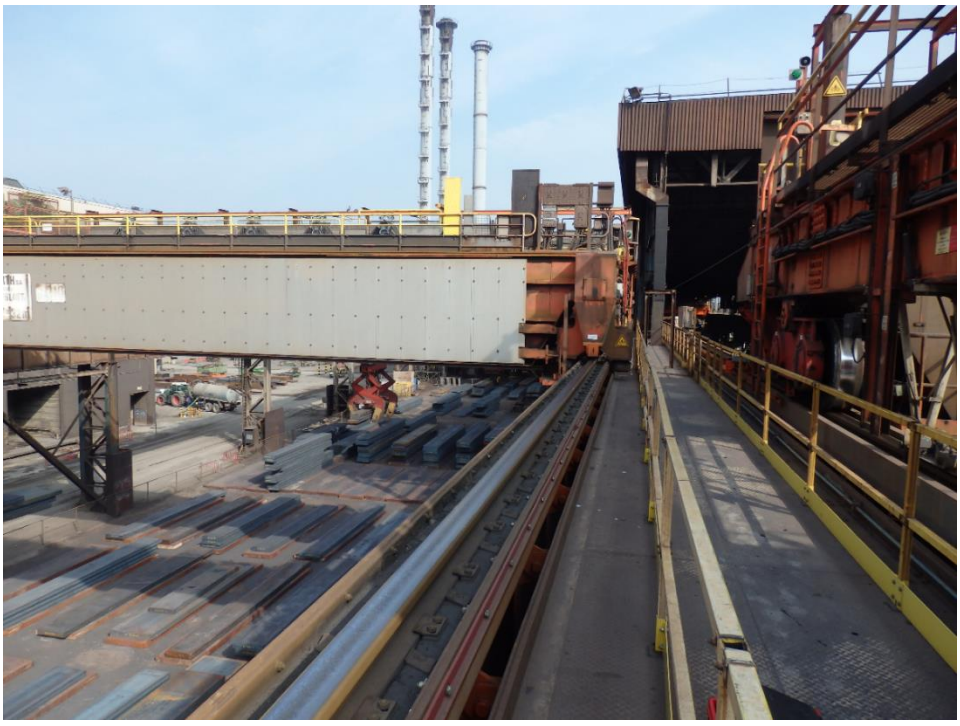

Figure 4.2 Rail were the crane moves forward and backwards.

Figure 4.3 First overhead crane analysed in the project.

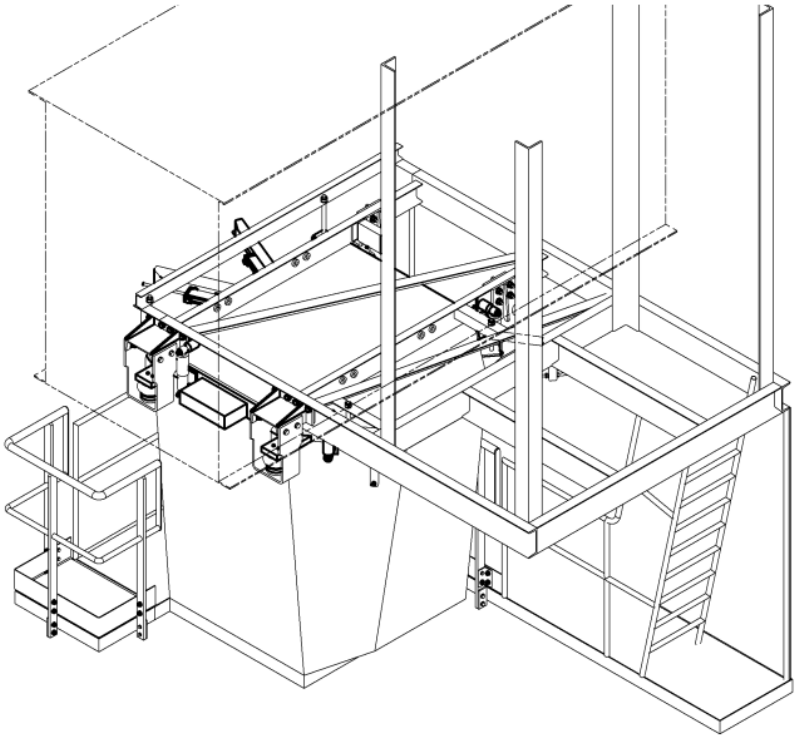

Figure 4.4 Isometric view of the first cabin. (Arcelor Mittal drawing.)

Figure 4.5 Grippers of the crane.

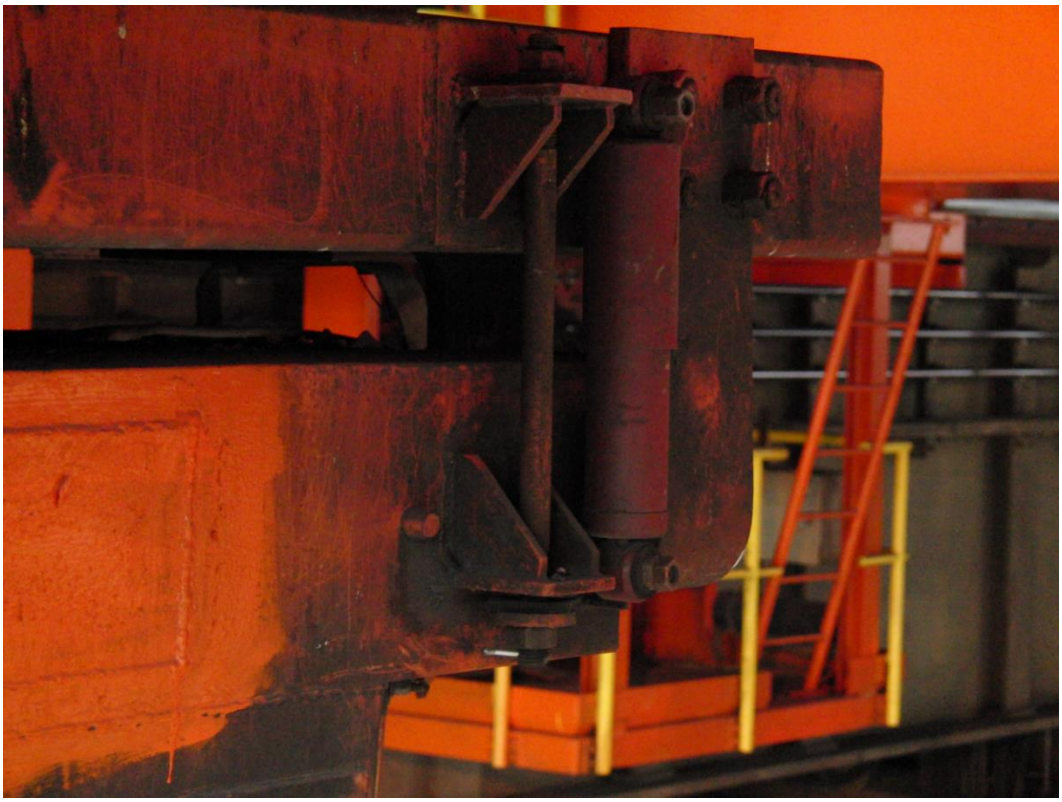

Figure 4.6 Present hydraulic dampers installed in the crane.

4.2 Field analysis

4.2.1 Introduction

During the testing days the company provided for all safety elements needed and an engineer of the company helped us, also a crane operator was in our disposition in order to perform the tests. In this apparat the whole field analysis inside and outside the cabin is explained starting with the tools used.

4.2.2 Tools and set up for the analysis outside the cabin

The first step in the evaluation of the current situation is the measurement of the incoming vibrations at the structure out of the cabin. To do so an L-shaped measuring device was constructed in which six K-Beam ® 8305A1M2 capacitive accelerometers of *Kistler* able to measure low-level, low-frequency vibrations and even static accelerations were placed, see figure 4.8 and figure 4.9. Using this method the six rigid body movements, three translations and three rotations, could be recorded by placing and fixing the measuring device on the structure outside the cabin. The fixed distances between the different accelerometers L1, L2 and L3 made it easy to calculate the rotations in all the directions. This method was proposed by Koen Deprez [24].
The before mentioned accelerometers were connected to a power box for their energy supply and also to a card in order to save the data acquisition that was recorded, see figure 4.7. A data acquisition card of the company *National Instruments 6346* was used for this task. Finally that card was connected to a computer in which using the interface of LabVIEW the data was saved in excel format.

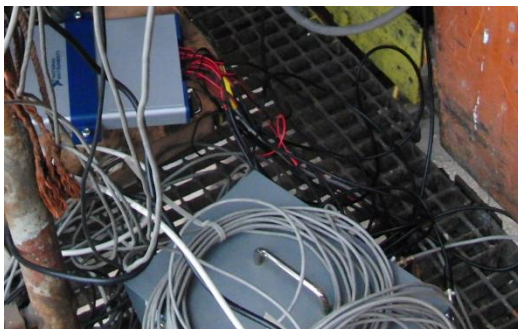

Figure 4.7 Data acquisition card on the top left and the power box in the bottom.

The position of the L-device was different in the two cranes and for that reason the values provided by each accelerometer changed between the two analyses. This had to be taken into account in order to calculate properly the rotations in each test. A picture of the device disposition in the second crane measurement is shown at figure 4.8.

Figure 4.8 L-shape measuring device in position at the second crane measurement.

Figure 4.9 Placement of the accelerometers in the L-shape measuring device.

The following equations give the expression for the angular accelerations in roll, (rotation around the x-axis) in pitch (rotation around the y-axis) and in yaw (rotation around the z-axis) for the first and second crane analysis. Equations (4.1) for the first crane and (4.2) for the second. The parameters referenced in this equations can be seen at Figure 4.10.

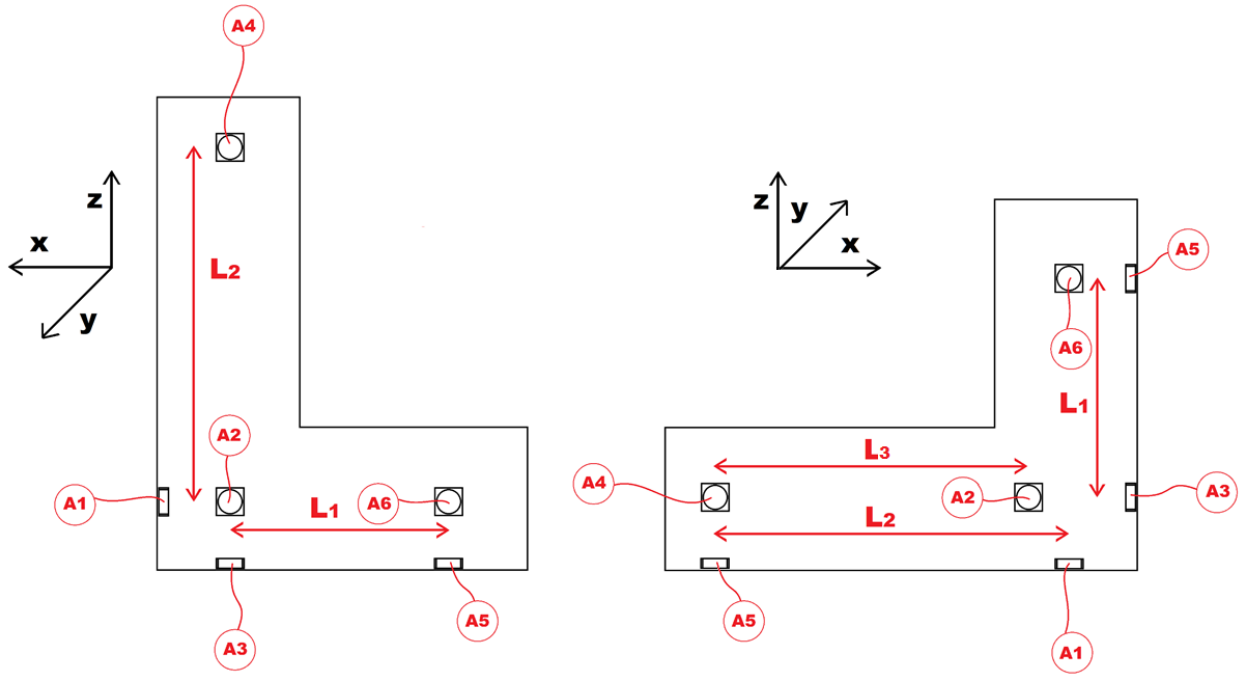

Figure 4.10 L-shape measuring device schema with six accelerometers and axis of the first crane measurement in the left and of the second crane in the right.

$$\begin{aligned} roll &\cong \frac{A_2 - A_4}{L_2} \\ pitch &\cong \frac{A_5 - A_3}{L_1} \\ yaw &\cong \frac{A_2 - A_6}{L_1} \end{aligned} \tag{4.1}$$

Where:

$$L_1 = 0.16m \quad L_2 = 0.24m$$

$$\begin{aligned} roll &\cong \frac{A_6 - A_2}{L_1} \\ pitch &\cong \frac{A_5 - A_1}{L_2} \\ yaw &\cong \frac{A_4 - A_2}{L_1} \end{aligned} \tag{4.2}$$

Where:

$$L_1 = 0.17m \quad L_2 = 0.25m \quad L_3 = 0.21m$$

4.2.3 Tools and set up for the analysis inside the cabin

The second step in the evaluation of the current situation of the overhead crane, is to measure the properties of the incoming vibrations inside the cabin. To do so also six K-Beam ® 8305A1M2 capacitive accelerometers of *Kistler* were placed, the ones used for translation movements are shown in Figure 4.11. In this part of the analysis the two cranes had the same physical distribution of accelerometers.

In the analysis of rotations an undefined error made the accelerometers placed for the calculation of the rotations give useless and random data values which ended in the impossible definition of the rotations inside the cabin of all the tests performed. The six accelerometers where connected to the computer using the same methodology explained in section 4.2.2.

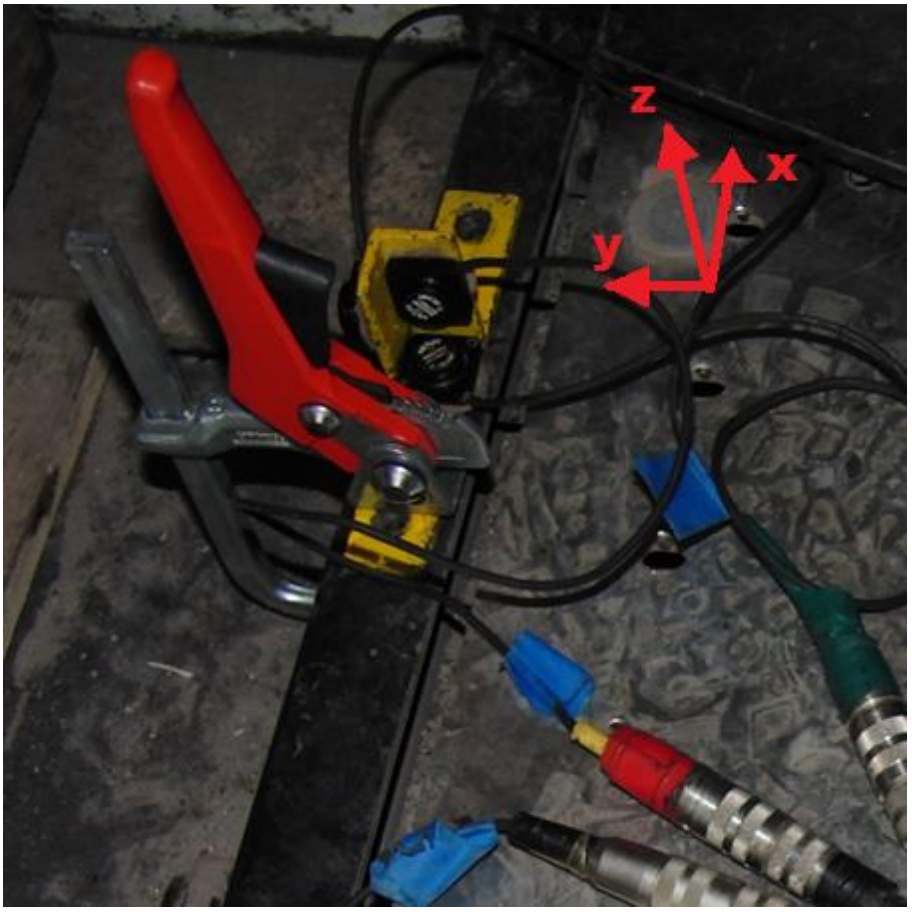

Figure 4.11 Accelerometers positioning inside the cabin for the recording of translation movements.

4.2.4 Tests performed

The tests performed were separated in different categories. All the measurements were performed at 20000Hz. First the operator was told to do the working movements that he would perform in a normal working day. Several tests of two minutes were made in order to analyse results with more accuracy. The result of this analysis will be compared to the analysis done before by the company AIB-VINÇOTTE international. Also this results were compared to the values used by the European directive to dictate the vibration exposure of the operators. So with this first tests a general comfort value analysis could be done.
Secondly the tests were more specific, making the operator do just *x* movements (the longitudinal direction in which the crane moves forward), *y* movements (lateral movements of the crane), *x* and *y* combined movements and finally pick up and let down the blocks with the grippers. In this way an analysis of which kind of vibration appears in which movement is done. Using this information it will be easier to design a better suspension for the crane. As said before in that second crane one of the leaf springs was broken and for that reason the cabin was fixed to the structure. The results can be significantly different from the ones of the first day as the suspensions are very different. At table 4.1 the different tests performed are listed.

Tests	Number	Description
First crane (General tests)	I	Test in general working conditions 1
	II	Test in general working conditions 2
	III	Test in general working conditions 3
Second crane (Specific tests)	IV	Test picking up the blocks
	V	Test picking up the blocks 2
	VI	Test downloading the blocks
	VII	Test driving in x direction without load 1 (fore and aft bridge drive)
	VIII	Test driving in x direction without load 2 (fore and aft bridge drive)
	IX	Test driving in y direction no load (lateral drive)
	X	Test driving in y direction (lateral drive) with load
	XI	Test driving x and y direction with load

Table 4.1 Vibration conditions tested on the overhead crane.

4.3 Analysis of the raw data

4.3.1 Introduction

The data obtained in the field had to be conditioned as it was only values in volts given by each of the accelerometers. One of the most complex and important parts of this project was the proper filtering, conditioning and analysing of the data including the calculation of the comfort values for each test. To do so the program Matlab was used in the whole process. In the annex A the Matlab code for doing all this is explained with detail. In this chapter it is given an overview of the process followed.

4.3.2 Filtering and conditioning

The first step was to import the excel data to the Matlab file, changing the format of comas used in excel for the dots used in Matlab. After that the average of the signal was removed obtaining only the variations around the static acceleration. See annex A.1.1. After, a low pass filter with cut-off frequency of 50 Hz was used in order to prevent aliasing. See the Matlab code for that at annex A.1.2.

The next step was resampling the data from 20000Hz to 200Hz in order to accelerate the data processing of the computer and clean the signal [24]. The next step of the conditioning was the transformation of the values in volts to acceleration knowing that in our configuration 0.5 Volts equal to 9.81 m/s^2. See annex A.1.1.

At this point the data was in the units that were needed for graphing the parameters in time domain. After plotting the accelerations the periods of time in which there was no signal were removed. A longer explanation of this process is explained in annex A.1.1.

Finally the data was in a proper way to analyse in frequency domain (Magnitude Spectrum and Power Spectral Density PSD). See annex A.2.1 for the code used in Matlab.

For the analysis of effRMS, crest, VDV and VDV8h a weighting filter was applied to the data used for the frequency domain analysis [7]. A longer explanation of the weighting filters applied and how the comfort values were obtained is explained in the Annex A.2.2.

4.3.3 Frequency domain analysis of the measurements

The first thing that is evaluated is the magnitude spectrum of the tests in *x*, *y* and *z* direction in and outside the cabin. To do so the Fast Fourier Transform (FFT) representation is used, see figure 4.12. It can be seen that the tests are full of shocks in a very large range of frequencies and that show that VDV values are the ones that will most certainly be used for the comfort evaluation. The code for the magnitude spectrum is explained in annex A.2.1.

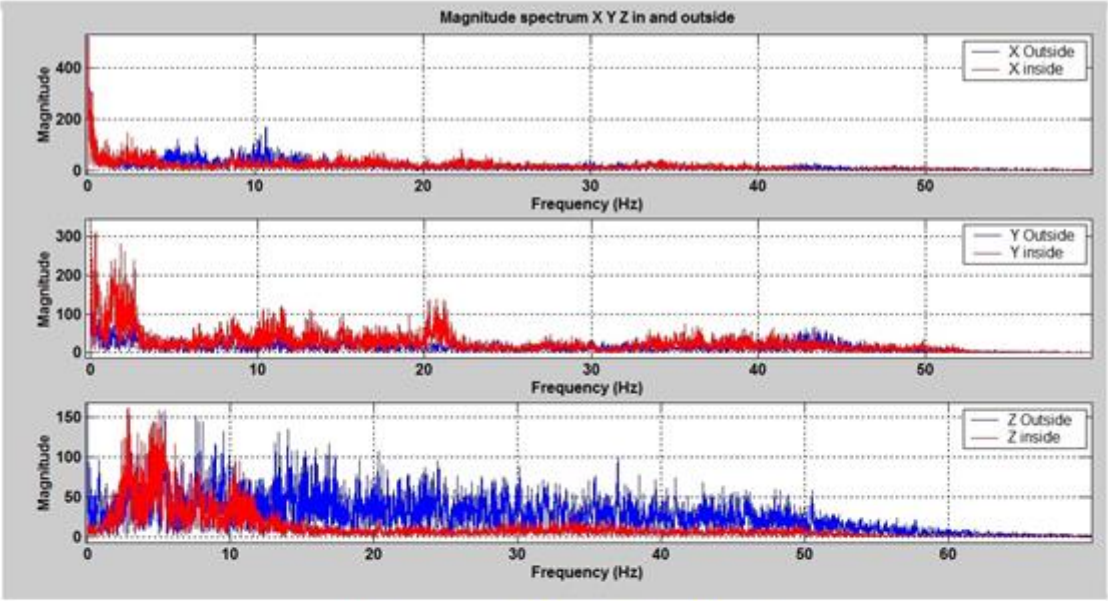

Plot from one of the tests of the first crane

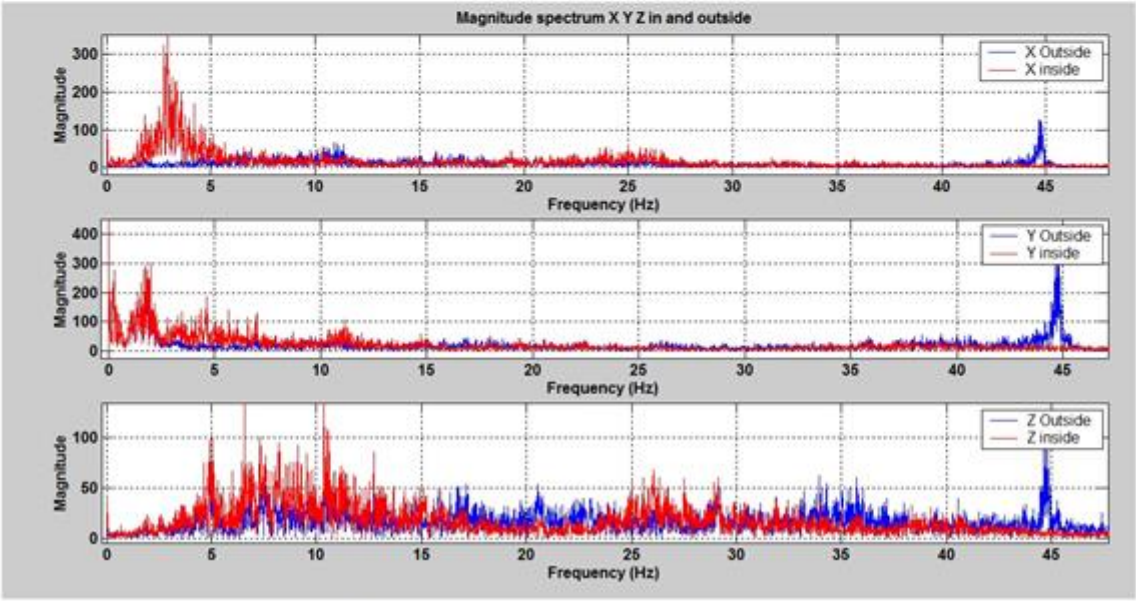

Plot form the test X of the second crane

Figure 4.12 Magnitude spectrum of two tests in *x*, *y* and *z* translations respectively.

Depending on the magnitude of the frequency between inside and outside the cabin (before and after the suspension), it can be confirmed if the suspension improves the situation, reducing the magnitude or it makes the problem worse amplifying the input signal.
The tests in the first crane, show improvement in the *z* direction starting at 15Hz. The suspension system response inside the cabin has an amplification of the vibration between 2 and 6 Hz, this indicates that the natural frequency (point with the maximum amplification in the suspension) could be around 3-4Hz in the *z* axis. In *x* and *y* axis the vibration isolation is inexistent, the response inside is worse than outside. This happens because the crane is only designed to perform well in *z* translation.
The input does not have any special frequency where it is needed to be careful. This is because as the signal is full of shocks and for that reason the design of a new suspension will not have any handicap in terms of natural frequencies. That also indicates that the input PSDs analysed later will be most likely flat and with not much information to give.

Looking at the tests in the second crane, the one with the leaf spring blocked, the results show that vibration isolation is inexistent as all translation vibrations are worse inside than outside the cabin. For that reason the solution of blocking the broken leaf spring to the structure is not a good solution.
It can also be clearly seen that in the tests of the second crane there is an important frequency magnitude amplification outside the cabin at 43 Hz which has an unknown origin. This crane needs an improvement because the amplification inside the cabin is quite big and the actual suspension only makes the problem of vibration worse. It can be confirmed looking at the frequencies of the input that there are no special issues to design a suspension regarding natural frequencies as the input signal has no clear dominant frequency until 35Hz.

The next step of the process was the calculation of the PSDs. They were calculated using 4096 points per window, with an overlap of 2048 points. To smooth the effect of leakage, a Hanning window was applied. These parameters were identically in every case to avoid disfiguring the results when comparing different measurements. With a sample frequency of 200Hz a frequency resolution of 200/4096 ≈ 0.05 Hz was obtained.

The PSD also reflect the attenuation that the suspension do to input vibrations but in a more clear way. It illustrates the frequencies that need to be attenuated and it also show clearly the effects that the suspension produce to the signal. With the PSD it is also easy to find the natural frequency of the suspension implemented and say how good is the attenuation starting in a specific frequency, see figure 4.13. The code for the PSD implementation is explained in annex A.2.1. In figure 4.14 and 4.15 it is shown the effect that the suspension of the first crane made to the signal.

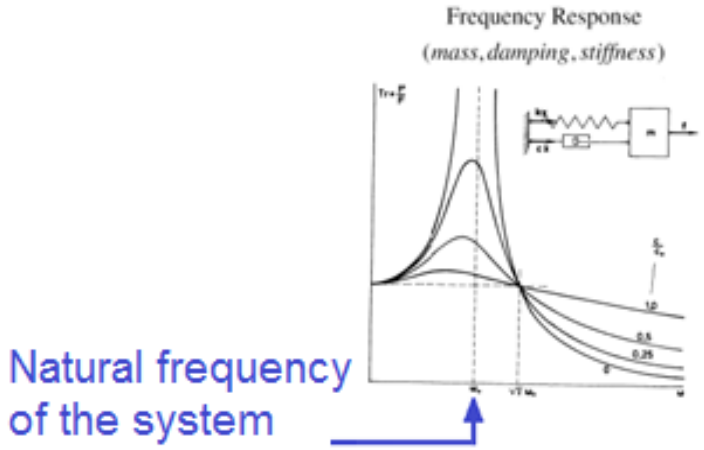

Figure 4.13 Theoretical plot of the attenuations that a suspension system can do at different frequencies.

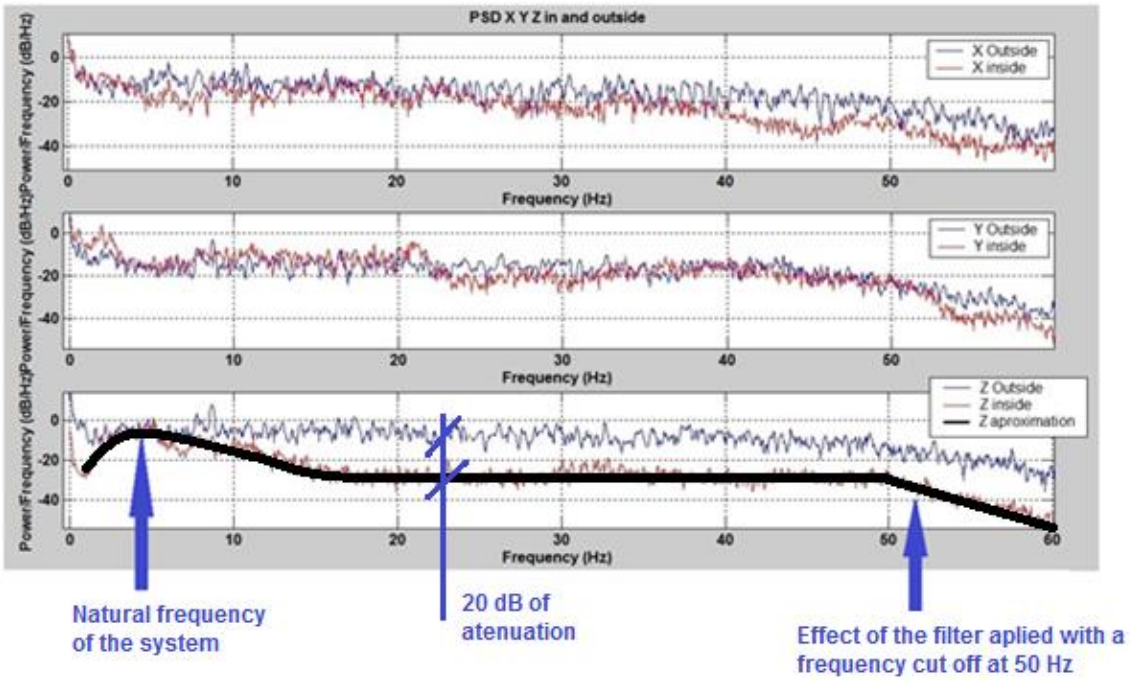

Figure 4.14 One of the PSD test in the first crane in X, Y and Z translation respectively.

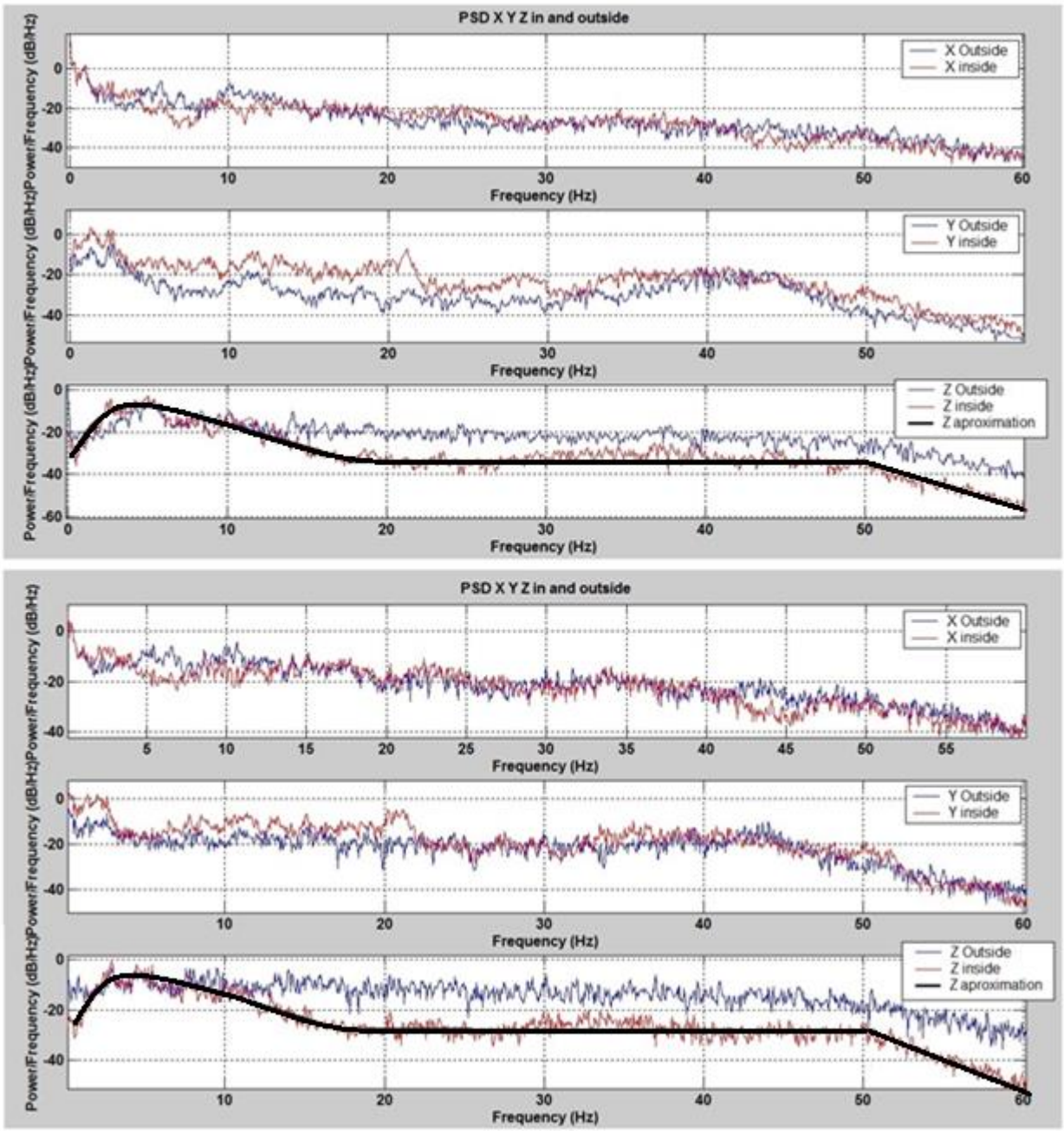

Figure 4.15 Two PSD tests in the first crane in *x*, *y* and *z* translation respectively.

In figures 4.14 and 4.15 an approximation of the *z* axis is done in order to interpret the results in a simpler way. It can be seen with that approximation that the natural frequency of the first crane suspension in the *z* axis is approximately of 3-4 Hz. The reduction of vibrations is of 20 dB more or less starting at 15-16 Hz. In *y* direction there is amplification of the vibration inside the cabin and in *x* there is no significant difference between inside and outside the cabin, this happens because the first crane is not prepared for the isolation of *x* and *y* vibrations.

The suspension of the first crane is not bad but could be improved implementing a suspension with a lower natural frequency with a good isolation of vibrations starting before than 15 Hz. It would be also interesting to apply some suspensions for the attenuation of the vibration in *x* and *y* translations.

The next step in the analysis is the interpretation of the PSD of the second crane, the one with the leaf springs, one of them broken and secured to the structure. See PSD at figure 4.16 and 4.17.

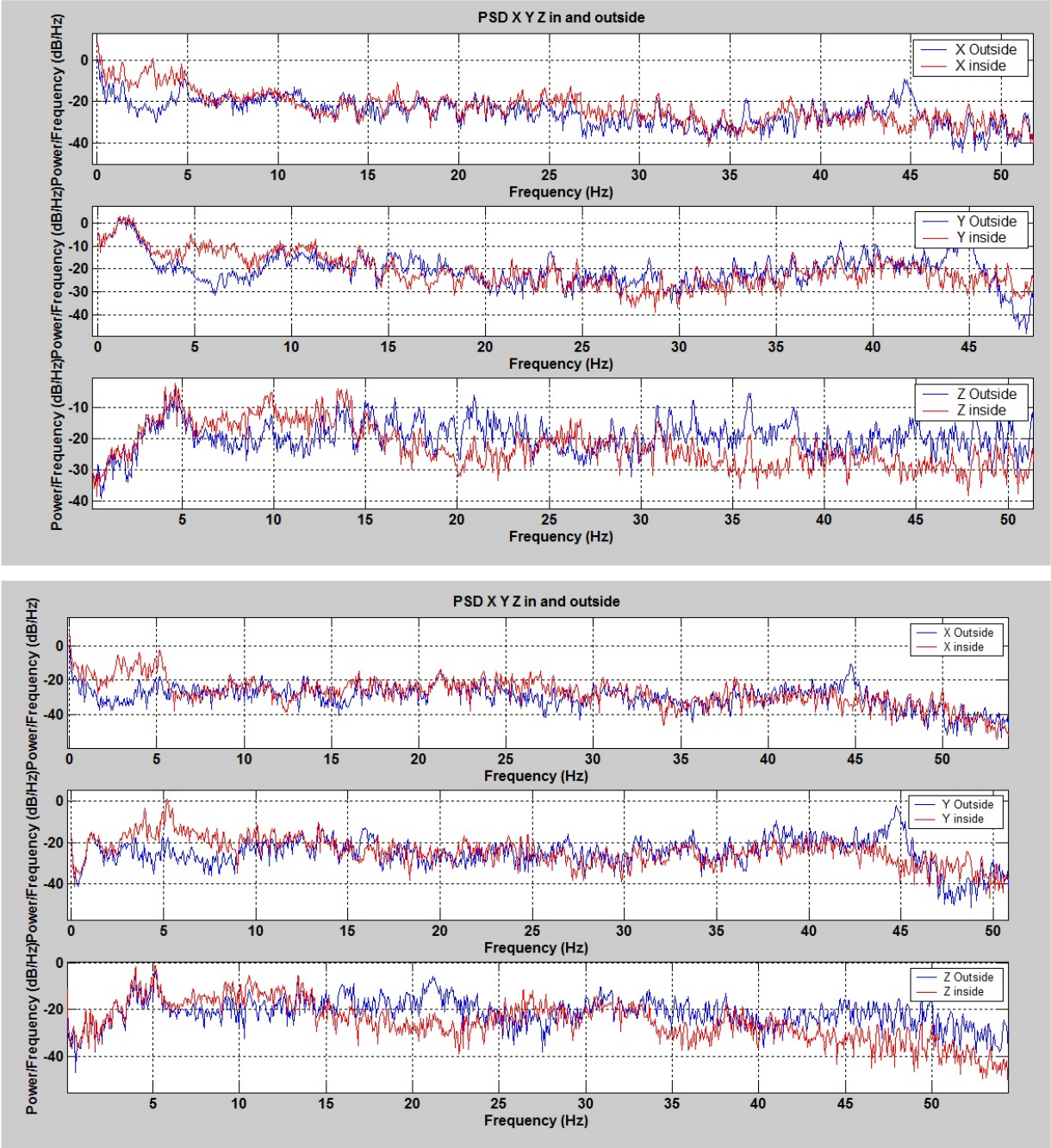

Figure 4.16 Two examples of the PSD of the second crane, tests IV and VII respectively.

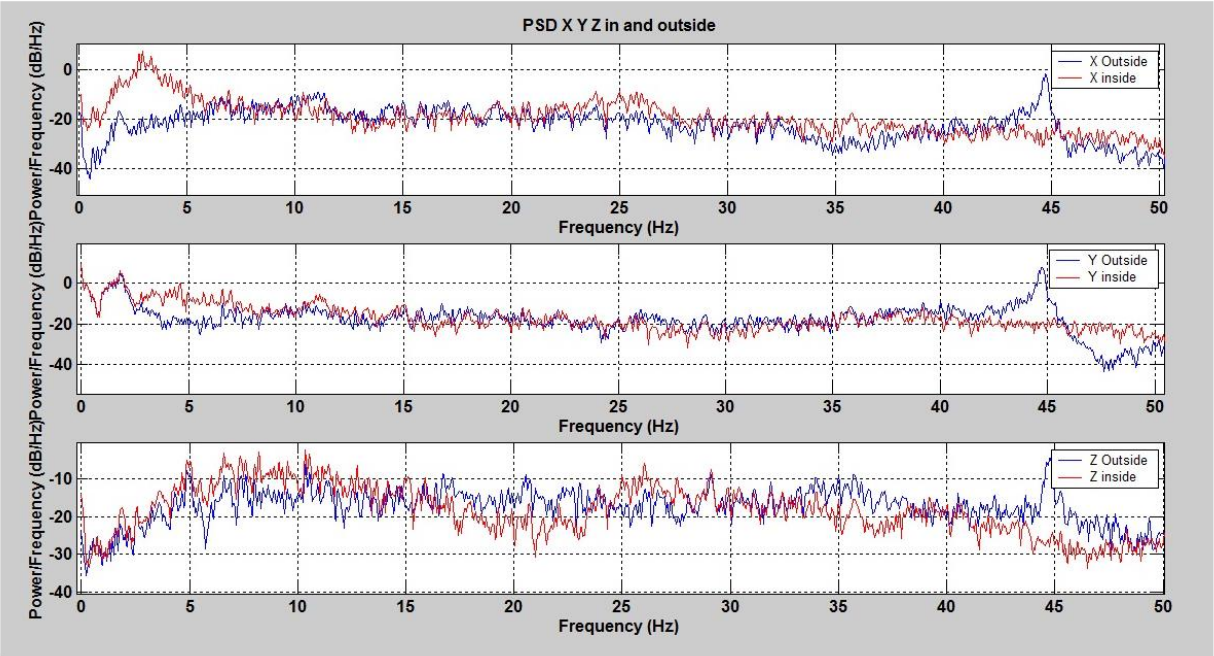

Figure 4.17 One of the PSD of the second crane, test X.

In the PSD of the second crane the input signal is really flat and this means that for the implementation of another suspension there is not a special frequency to take care of as the input vibration has not dominant frequencies. This is good for our future suspension design, as no special frequency has to be taken care off. However this is bad for the interpretation of the input frequencies as if it is so full of shocks and so flat, it is impossible to distinguish which frequencies could be result of which movements in the different plots of the tests performed.

The only thing that can be seen in the tests as a major tendency is that until 5 Hz the frequency graphic in and out is almost the same, this can make us think that the inside and outside of the cabin move together in low frequencies, logical conclusion knowing that one of the leaf springs is blocked within the structure. It can also be seen in some tests that there are two dominant frequencies one around 10 Hz and the other at 25 Hz approximately. The first one could be the natural frequency of the suspension system and the other could be the natural frequency of the structure which it is not an element with infinite stiffness, but this theory can not be clearly demonstrable as this behaviour is not constant in all the tests.

4.3.4 Time domain analysis of the measurements

A fast look to the acceleration plots show the difference between the tests made in the first crane, were it can be clearly seen that the suspensions are reducing the accelerations inside the cabin, and the ones of the second crane, in which the vibration inside the cabin is even worse than outside, see figure 4.18.

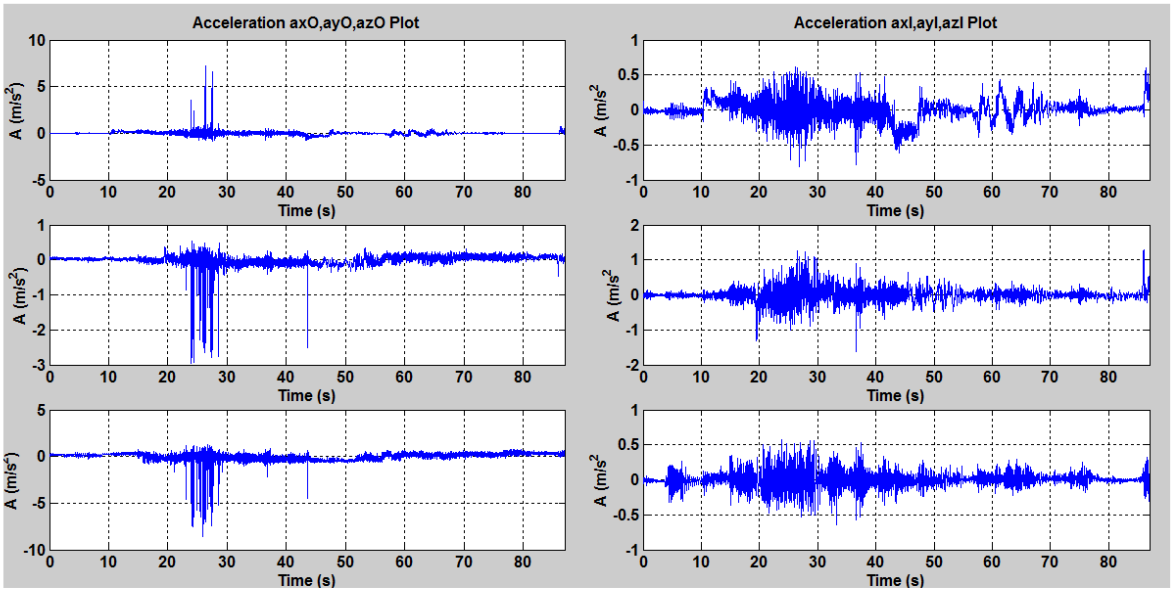

Plot from a test of the first crane

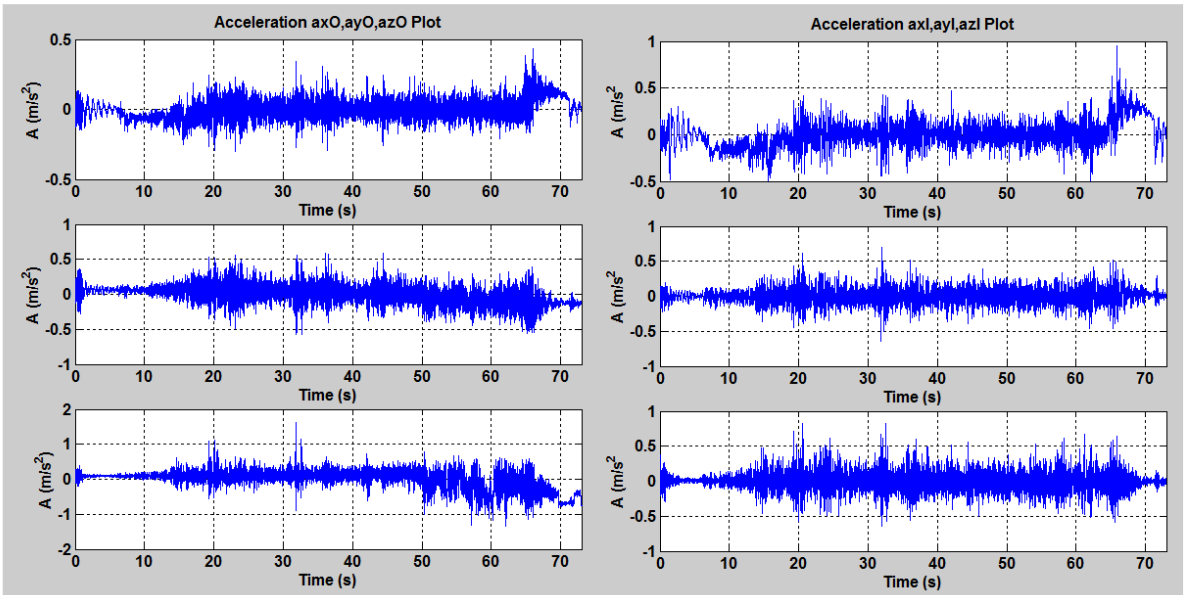

Plot form a test of the second crane

Figure 4.18 Comparison between acceleration plots from the two cranes.

The most important part of our time domain analysis is the calculation of the effRMS, crest, VDV and VDV8h which are later compared to the values given by the normative. The first step is the implementation of the weighting filter applied to the data used for the frequency domain analysis. This filter put emphasis on those frequencies that are particularly harmful and filter out the ones of less importance. This knowledge is obtained through epidemiologic studies that show that the sensitivity of the human body to vibration depends greatly upon the direction of the vibration [7].

The filters used are the weighting filters of the BS6841 [29]. There are different filters, one for *z* translation (4.1), another for *x* and *y* translations (4.2) and finally another one for rotations (4.2).

$$W_i(s) = \frac{(s + 2\pi f_3)\left(s^2 + \frac{2\pi f_5}{Q_3}s + 4\pi^2 f_5^2\right)}{\left(s^2 + \frac{2\pi f_4}{Q_2}s + 4\pi^2 f_4^2\right)\left(s^2 + \frac{2\pi f_6}{Q_4}s + 4\pi^2 f_6^2\right)} \cdot \frac{2\pi K f_4^2 f_6^2}{f_3 f_5^2} \qquad (4.1)$$

$$W_j(s) = \frac{(s + 2\pi f_3)}{\left(s^2 + \frac{2\pi f_4}{Q_2}s + 4\pi^2 f_4^2\right)} \cdot \frac{2\pi K f_4^2}{f_3} \qquad (4.2)$$

In which f_3, f_4, f_5, f_6, Q_2, Q_3, Q_4 and K are the parameters depending on the direction of the vibration, the orientation of the body and the place where the vibration is measured. For the filter of the equation (4.1), the parameters are the following: f_3=16, f_4=16, f_5=2.4, f_6=4, Q_2=0.55, Q_3=0.9, Q_4=0.95 and K=0.4 [29]. This filter is used for the vertical accelerations measured at the seat surface for a person in a seated posture. The second filter, based on equation (4.2) with f_3=2, f_4=2, Q_2=0.63, and K=1 is used for the fore and aft, and lateral accelerations of a seated person [29]. It can be seen that for the vertical direction the most important region is between 4 and 8 Hz where the weight is above one, while in the fore-aft and lateral direction, the frequency range of 0.5-2Hz has the largest weight [24]. The highest discomfort is allocated to the frequency ranges in which the human spine is most sensitive. Finally for the rotations, based also in equation (4.2) the values are f_3=1, f_4=1, Q_2=0.63, and K=1 [29]. A magnitude representation of this filters it's shown at figure 4.19. The code used in Matlab can be seen at the annex A.2.2. Similar filters are used by the ISO standards, but those are more complicated to use and for that reason are not used in this project [24].

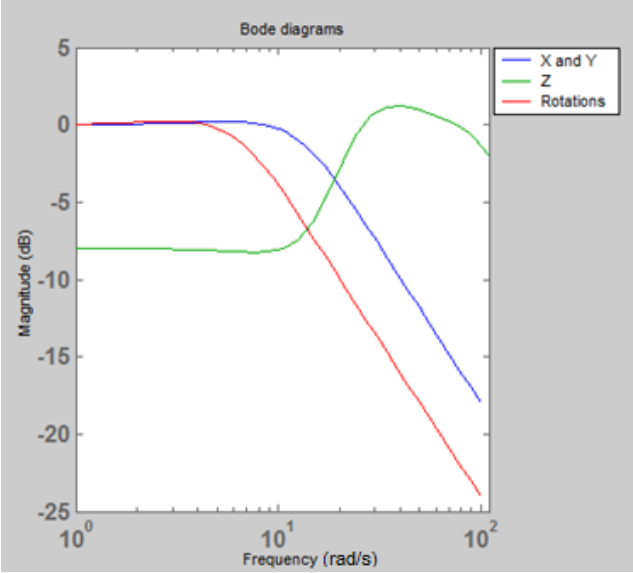

Figure 4.19 Bode magnitude diagram of the weighting filters used.

Once filtered, the data is in a proper format for calculating the effRMS (4.3), VDV (4.4), VDV8h (4.5), and crestfactor (4.6).

The effRMS is given by:

$$effRMS = \left[\frac{1}{N}\sum_{n=1}^{n=N} a_w^2\right]^{\frac{1}{2}} \tag{4.3}$$

With *N* being the number of points and a_w the frequency weighted acceleration data. The unit of effRMS is m/s^2.

The VDV is given by:

$$VDV = \left[\frac{T_s}{N}\sum_{n=1}^{n=N} a_w^4\right]^{\frac{1}{4}} \tag{4.4}$$

Being T_s the measurement period and *N* and a_w the same as defined before. The unit of VDV is $m/s^{1.75}$. This value is weak especially for periods of exposure below one minute because it does not contemplate the length of the measurement. For that reason the VDV8h is calculated as it takes in to account the time factor.

The parameter VDV 8h is given by:

$$VDV8h = \left(\frac{8 \cdot 3600 \cdot VDV^4}{\frac{N}{f_s}} \right)^{\frac{1}{4}} \tag{4.5}$$

This parameter is very useful for comparing the VDV of all the samples as it is referred to a single amount of time, eight hours and make it easier to compare results from different tests of different durations.

In numerous cases the RMS of the frequency weighted accelerations is a useful indicator of the severity of the vibrations but, if the vibrations are non-stationary or include a large number of shocks, the VDV8h is a better indicator. If the crest factor it is lower than 7 then we can consider that the vibrations are stationary thus we can use de RMS as a good indicator, if not, the VDV8h is the indicator to look at [7].

For obtaining the crest factor the next equation is used:

$$Crestfactor = \frac{a_{max}}{effRMS} \tag{4.6}$$

Where a_{max} is the maximum peak acceleration. This factor is usually calculated from the acceleration after it has been frequency weighted.

As mentioned in the section 2.4 the daily exposure limit value is set to an effRMS of 1.15m/s^2 or a VDV of 21 m/s$^{1.75}$ over an eight-hour reference period and the daily action value is for that same eight-hour period at an effRMS of 0.5m/s^2 or a VDV of 9.1 m/s$^{1.75}$, see table 4.2. This values can not be violated and once they are, the company has to implement a technical program to reduce the exposure to vibrations [5].

The values of table 4.2 are only for translation movements as the rotations are calculated differently. In the tables 4.3, 4.4 and 4.5 the values of RMS, crestfactor, VDV and VDV8h from each test are listed.

If crestfactor in translation is	
<7	>7
Then effRMS max	Then VDV8h max
0.5 m/s^2	9.1 m/s$^{1.75}$

Table 4.2 Maximum legal values for an eight-hour period of a daily working environment in translations.

Nº	X Outside the cabin				X Inside the cabin				Rotation X Outside the cabin			
	Eff RMS [m/s^2]	Crest	VDV [m/s$^{1.75}$]	VDV 8h [m/s$^{1.75}$]	Eff RMS [m/s^2]	Crest	VDV [m/s$^{1.75}$]	VDV 8h [m/s$^{1.75}$]	Eff RMS [rad/s^2]	Crest	VDV [rad/s$^{1.75}$]	VDV 8h [rad/s$^{1.75}$]
I	0.151	2.975	0.652	2.680	0.148	2.872	0.638	2.623	0.478	7.616	3.223	13.244
II	0.106	9.008	0.545	2.326	0.100	3.629	0.493	2.102	0.677	6.145	3.590	15.314
III	0.104	2.970	0.515	2.090	0.101	2.793	0.499	2.026	0.643	6.514	3.927	15.944
IV	0.039	2.620	0.179	0.830	0.100	2.523	0.440	2.036	0.057	5.497	0.228	1.056
V	0.008	11.958	0.064	0.302	0.031	8.371	0.185	0.873	0.031	10.569	0.222	1.050
VI	0.021	4.354	0.079	0.401	0.078	5.328	0.319	1.616	0.034	3.759	0.121	0.613
VII	0.020	3.539	0.076	0.372	0.052	3.845	0.194	0.952	0.048	4.027	0.190	0.933
VIII	0.044	4.348	0.202	0.902	0.108	4.250	0.487	2.171	0.291	1.758	1.013	4.514
IX	0.014	7.418	0.065	0.292	0.068	5.037	0.290	1.298	0.302	1.734	1.052	4.703
X	0.014	7.642	0.063	0.283	0.062	5.135	0.274	1.220	0.108	3.758	0.473	2.108
XI	0.044	4.170	0.184	0.872	0.110	3.530	0.453	2.147	0.044	4.871	0.173	0.820

Table 4.3 Comfort values for translation and rotation X.

Nº	Y Outside the cabin				Y Inside the cabin				Rotation Y Outside the cabin			
	Eff RMS [m/s^2]	Crest	VDV [m/s$^{1.75}$]	VDV 8h [m/s$^{1.75}$]	Eff RMS [m/s^2]	Crest	VDV [m/s$^{1.75}$]	VDV 8h [m/s$^{1.75}$]	Eff RMS [rad/s^2]	Crest	VDV [rad/s$^{1.75}$]	VDV 8h [rad/s$^{1.75}$]
I	0.027	5.821	0.178	0.733	0.071	9.653	0.453	1.861	0.521	10.149	3.458	14.210
II	0.083	2.335	0.360	1.536	0.089	7.168	0.518	2.208	1.773	4.606	6.905	29.453
III	0.040	5.890	0.245	0.994	0.099	7.590	0.586	2.378	0.688	7.387	4.096	16.63
IV	0.083	4.985	0.388	1.796	0.092	5.002	0.427	1.975	0.656	5.458	3.055	14.126
V	0.012	7.279	0.065	0.305	0.024	10.40	0.160	0.758	0.318	4.382	2.179	10.284
VI	0.053	5.766	0.256	1.297	0.063	5.026	0.294	1.490	0.556	4.620	2.258	11.422
VII	0.011	4.595	0.040	0.196	0.021	5.260	0.085	0.419	0.126	4.409	0.478	2.340
VIII	0.071	1.963	0.247	1.102	0.028	5.157	0.120	0.536	1.329	3.519	5.877	26.192
IX	0.111	4.847	0.481	2.152	0.115	4.590	0.504	2.253	1.768	2.669	5.787	25.879
X	0.112	4.200	0.507	2.261	0.120	4.576	0.551	2.454	0.786	4.457	3.683	16.416
XI	0.020	8.076	0.105	0.497	0.032	6.806	0.142	0.675	0.270	5.447	1.062	5.036

Table 4.4 Comfort values for translation and rotation Y.

Nº	Z Outside the cabin				Z Inside the cabin				Rotation Z Outside the cabin			
	Eff RMS [m/s^2]	Crest	VDV [m/s$^{1.75}$]	VDV 8h [m/s$^{1.75}$]	Eff RMS [m/s^2]	Crest	VDV [m/s$^{1.75}$]	VDV 8h [m/s$^{1.75}$]	Eff RMS [rad/s^2]	Crest	VDV [rad/s$^{1.75}$]	VDV 8h [rad/s$^{1.75}$]
I	0.074	6.916	0.761	3.128	0.083	5.835	0.411	1.690	0.717	7.616	4.835	19.867
II	0.293	4.987	2.736	11.67	0.098	5.480	0.482	2.055	1.015	6.145	5.385	22.971
III	0.151	6.637	1.520	6.171	0.111	6.060	3.927	2.211	0.965	6.514	5.891	23.917
IV	0.075	9.310	0.385	1.782	0.101	9.755	0.505	2.334	0.085	5.497	0.343	1.585
V	0.096	11.63	0.678	3.201	0.130	11.06	0.932	4.398	0.047	10.569	0.334	1.575
VI	0.144	9.558	0.821	4.152	0.188	10.41	1.086	5.495	0.052	3.759	0.182	0.920
VII	0.074	6.449	0.319	1.563	0.086	4.810	0.342	1.676	0.072	4.027	0.286	1.400
VIII	0.152	6.648	0.674	3.005	0.118	5.257	0.510	2.275	0.437	1.758	1.520	6.771
IX	0.132	4.210	0.493	2.204	0.123	6.826	0.580	2.596	0.453	1.734	1.577	7.055
X	0.077	6.111	0.358	1.596	0.112	6.800	0.521	2.322	0.162	3.758	0.709	3.162
XI	0.110	8.240	0.477	2.263	0.127	4.417	0.514	2.435	0.066	4.871	0.259	1.230

Table 4.5 Comfort values for translation and rotation Z.

The values of the first day, taken in normal work conditions are quite resembling with the test made for the other company, see the other test in annex C. In the test of the second day the values are lower because there is no combination of multiple actions and therefore the results are lower, inside the cabin the values are worse than outside in most of the cases but none of them is even close to the limit values. For a better understanding of the numbers a graphical representation of the RMS and VDV8h is shown in figure 4.20.

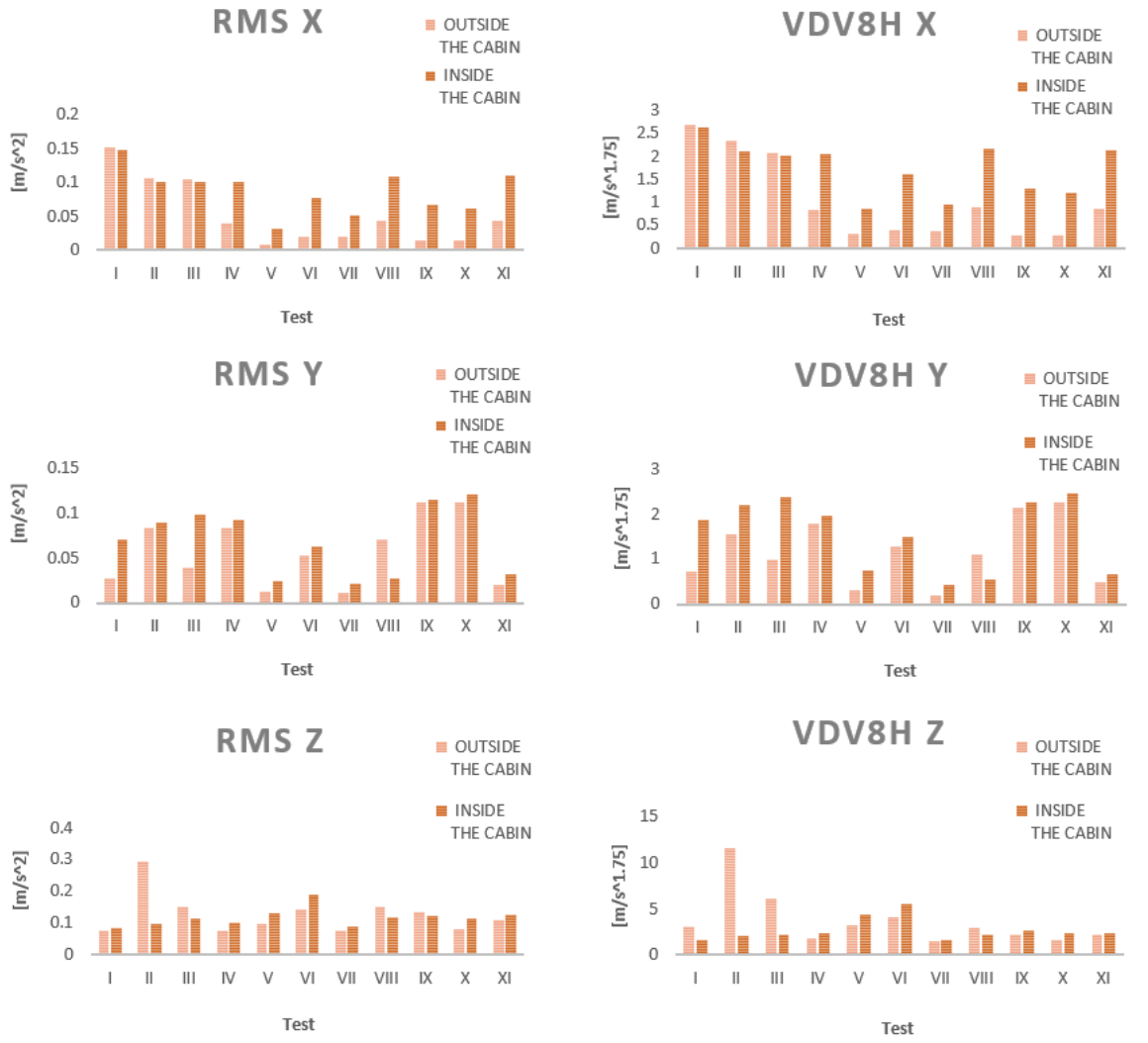

Number	Description
I	Test in general working conditions 1
II	Test in general working conditions 2
III	Test in general working conditions 3
IV	Test picking up the blocks
V	Test picking up the blocks 2
VI	Test downloading the blocks
VII	Test driving in x direction without load (fore and aft bridge drive) 1
VIII	Test driving in x direction without load (fore and aft bridge drive) 2
IX	Test driving in y direction (lateral drive) with no load
X	Test driving in y direction (lateral drive) with blocks
XI	Test driving x and y direction with load

Figure 4.20 Graphical representation of the RMS and VDV8h for all the tests.

In the figure 4.20 the difference between the three first tests, done in the crane with normal working conditions, and the rest of the tests, done in specific working conditions, can be seen. The results of the first crane (I, II and III) show that the suspension is working properly in *z* translation, at *x* it is not doing much improvement and in *y* it is amplifying the vibrations. So, in the new suspension a better isolation of the frontal and most importantly lateral movement needs to be done.

In the specific tests of the second crane it can be clearly seen that the isolation inside it is worst that outside so, the temporal solution of blocking one of the leaf springs it's not a good solution to the problem as mentioned before. It can also be noticed that the *x* translation is much worse inside than outside the cabin, in *y* and *z* translations there is the same problem but not that exaggerated. As it is logical it can also be seen that when picking blocks and downloading them is when the biggest *z* vibrations appear. When the driver goes laterally there is more *y* vibrations but when the driver combines lateral and fore and aft movements the *y* vibrations seem to get lower so the major problem is with lateral movement alone.

The values of effRMS for rotations can be compared to the vibration measurements in the seat of a driver of a tank over a rough cross-country course [7]. The values are r_x=0.442 rad/s^2, r_y=0.786 rad/s^2 and r_z=0.104 rad/s^2. With this values a general overview of the expected magnitude of the values can be formed as the normative does not give limit values for rotation. With this comparison the values in the r_x and r_z rotation in the first crane are clearly bigger than the ones from the tank, in the second crane the values are similar to the ones given in the tank. For r_y there are only two tests in which the values are bigger, one from the first crane and one from the second one. So, reminding that the values are inside the cabin of the tank, the only remarkable thing for the whole rotation comparison is that in the first crane, at rotation x, the values are ten times bigger than the ones from the tank and that may be a problem.

4.4 Conclusion

After finishing the analysis it can be appreciated that a need for the improvement of the vibration exposure of the operators is real. This is a confirmation of the results that the company AIB-VINÇOTTE International got, see annex B.

The tests made in the first crane, the one with air spring suspensions, pointed out that the natural frequency of the installed system was at 3 Hz approximately. The analysis out of the first cabin gave an unexpected result as the whole signal was composed of constant shocks in which no specific frequency had a bigger implication than another. This was not a bad result because it mean that there was not a dominant frequency in the excitation vibration. This gives the freedom to design a new suspension without having to worry about their natural frequency.

The specific tests made in the second crane for evaluating the possible frequency implications of each movement of the crane were not useful as all the tests where just a big amount of shocks. In the second crane studied, the analysis inside the cabin showed that the solution of blocking the broken leaf spring was not a good idea. The discomfort when driving this crane was bigger than with the first one and for that reason the need of an improvement is even more important than in the first one. As said before the analysis outside the cabin also pointed out that the system had a vibration environment composed with constant shocks in which no specific frequency had a bigger implication than another. For that reason there is a huge number of possibilities for the design and improvement of the situation.

As the company didn't gave specific parameters of the system like the (mass, stiffness or damping of the cranes studied) a transfer function could not be defined to see if a theoretical model would match the obtained results. It is only known that there is no special frequency excitation of the system.

Chapter 5

Development of a suspension system

In this chapter the proposal of a suspension system is done thanks to the analysis performed before in the cranes. A suspension system is chosen, explained and finally modelled using the extension Simulink of the platform Matlab. After that, the model is tested and used for knowing which would be the response of the system. Finally an interpretation of the results and an evaluation of the suspension system proposed is made.

5.1 Introduction

After looking at the results of the previous chapter a suspension system composed of four air springs with external air reservoirs could be a good, cheap and easy solution to install as it pointed out good results in other applications before [24],[32]. It also would fit well in the crane without having to change many things and for that reasons the company decided to give it a chance.

This system is really flexible as with the change of the opening in the throttle valve that connects the air spring with the external reservoir the stiffness and response of the air spring can be easily changed. This permits to get a really good isolation from the shocking environment with a system whose natural frequency is always low.

See figure 5.1 for a schematic overview of the system reduced to a one air spring with his external reservoir. The main chamber is linked with the external reservoir using a throttle valve. When the system receives a *x* input the main chamber of the air spring compresses or pulls so the air pressure P_1 changes. The change in air pressure creates an imbalance between the main chamber and the additional chamber, and the air flow through the throttle valve. When the high pressure air flows through the valve the flow creates damping which kill the vibration of the *y* output of the system. The opening of the throttle valve has a large relation to the damping and therefore when the model is created

it is necessary to make some tests with different valve openings to see which one gives is the most favourable response [24],[33]. The variables P, V, T and *p* are used on the hydromechanics and aerodynamics basic equations to create the model.

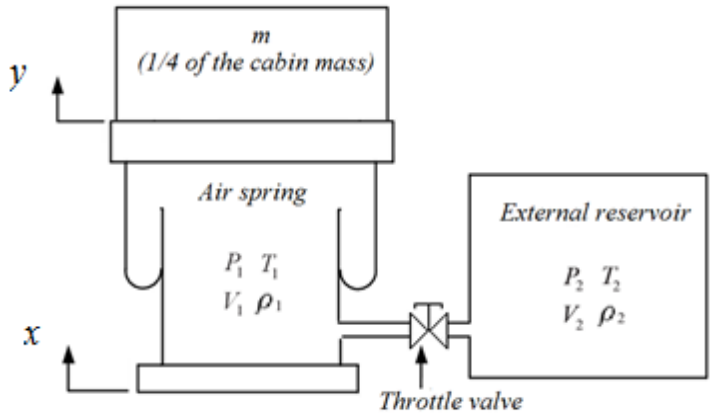

Figure 5.1 Basic schema of an air spring with an external reservoir suspension system. (P_i pressures, V_i volumes, T_i temperatures, ρ_i densities, *x* and *y* positions of respectively ground and mass m)

5.2 Pneumatic suspension system modelling

The next step in the process is modelling this proposed suspension system using the necessary hydromechanics and aerodynamics equations with the addition of specific parameters given by the company regarding the physical characteristics of a cabin. This model has been developed and used before by Koen Deprez [24]. The air spring selected for this first model is a Firestone Airstroke Airmount 131-M58-6155 [31] with an external reservoir of 37.5l. The selected model is this as one crane has incorporated this air spring model already and it will be easier to install just an external reservoir and do some tests. The aim of our model is to show the *y* response for an *x* vibration so, the first thing that has to be done is deriving the transfer function between vibration *y* and *x*. In order to do so the movement of the mass m is described by Newton's second law:

$$m\ddot{y} = (P_1 - P_0)A - mg \qquad (5.1)$$

With:

m	mass	P_1	pressure in air spring
$\ddot{y}$	acceleration of mass m	A	effective area of air spring
P_0	ambient pressure	g	gravitational acceleration

Generally the effective area A of an air spring is not a constant, it is function of the height and the internal pressure of the spring however, using the charts given by the manufacturing air spring company the effective area can be easily found and can be considered as a constant [31].
Considering this the spring volume V1 can be described through the following equation:

$$V_1 = V_{10} + (y - x)A \tag{5.2}$$

In which V_{10} is the volume of the spring when the system is at rest, value that can also be found using the charts given by the manufacturing company [31]. The volume of the auxiliary reservoir V_2 is constant and in our design its volume is set up at six times bigger than V_{10}. The only unknown parameter in equation 5.1 is P_1. To find this pressure the energy states of the air spring and of the auxiliary reservoir are formulated [24].
The conservation of energy of open systems states that the energy inflow minus the energy outflow equals the rate at which energy is stored inside a certain control volume. In our particular case the two enclosures, the spring and the auxiliary reservoir, are considered both as control volumes. All mass flowing from one control volume enters the other and vice versa and is represented by $\dot{m}$. Since there are no substantial height differences and changes in fluid speed, energy flow can be described by the enthalpy *h*. Assuming further that changes to the system happen instantly the heat flow of the system can be eliminated. All this changes lead us to the equation 5.3 where the first term indicates the energy flow to the control volume, the second the work done by the system and the third term the total internal energy in the system [24].

$$C_p \dot{m} T - P \frac{dV}{dt} = \frac{d}{dt}(C_v \rho V T) \tag{5.3}$$

With: C_p specific heat at constant pressure
T temperature (K)
V volume
C_v specific heat at constant volume

An expression for the mass flow in the system is found by relating the mass flow through the throttle valve to the pressure over it and that for a compressible fluid [34]. The mass flow is considered to be positive going to the auxiliary reservoir [24].

$$\dot{m} = \frac{d}{dt}(\rho_2 V_2) \tag{5.4}$$

$$\dot{m} = S\sqrt{2\rho_2 P_2 \left(\frac{\kappa}{\kappa - 1}\right)\left[\left(\frac{P_1}{P_2}\right)^{\frac{2}{\kappa}} - \left(\frac{P_1}{P_2}\right)^{\frac{\kappa+1}{\kappa}}\right]} \tag{5.5}$$

With: κ ratio of specific heats
S surface of valve opening

Applying equation 5.3 to both control volumes results in:

$$-C_p \dot{m} T_1 - P_1 \frac{dV_1}{dt} = \frac{d}{dt}(C_p \rho_1 V_1 T_1) \tag{5.6}$$

$$C_p \dot{m} T_2 = \frac{d}{dt}(C_p \rho_2 V_2 T_2) \tag{5.7}$$

With index $_1$ indicating the spring properties and index $_2$ the properties of the auxiliary reservoir. Combining equations 5.1, 5.2, 5.5, 5.6 and 5.7 with the law for ideal gases $(PV = mRT)$ a model of the system using Matlab Simulink can be created and simulated with different valve openings [24]. See Annex B.1 for the explanation of the non-linear model and plotting of the response. In figure 5.2 the results obtained running the simulation with different valve openings are shown.

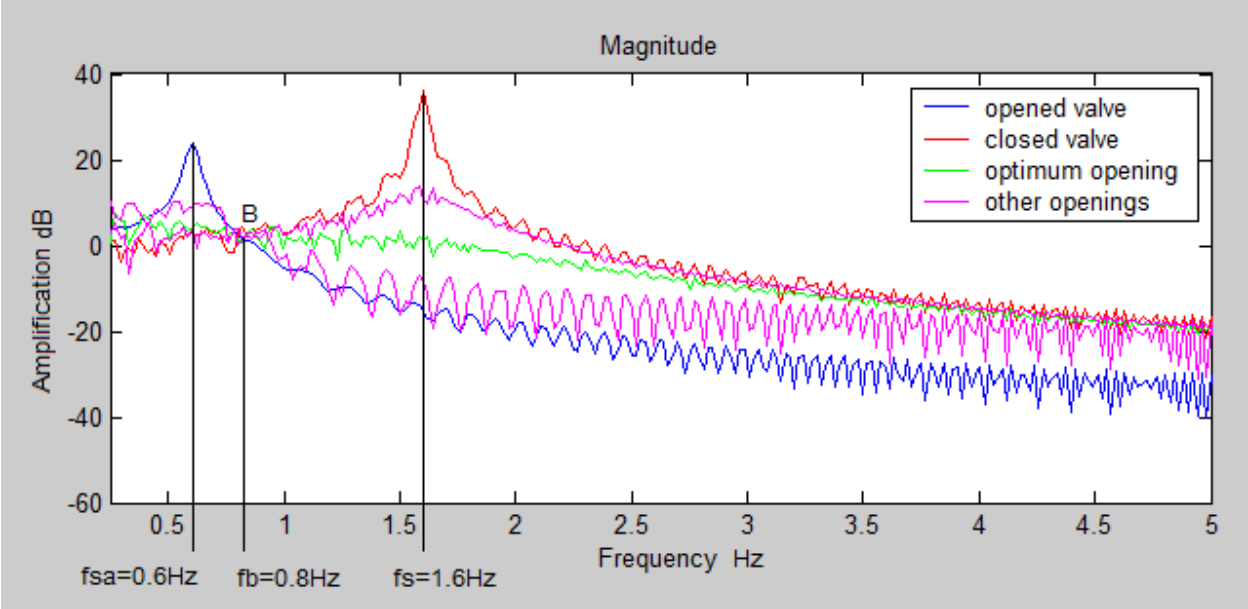

Figure 5.2. Simulated Frequency Response Function for different valve openings.

Figure 5.2 shows the frequency response function of the model using the air spring Firestone Airstroke Airmount 131-M58-6155 [31] with an external reservoir of 37,5l in various valve openings. The frequency response functions are obtained by exciting the system with a swept sine signal between 0.2 and 5Hz with an amplitude of 1,5cm [24]. The natural frequency of the air spring f_s, can be seen in the figure 5.2. The natural frequency of the air spring with the external reservoir can be also seen also in the figure 5.2 as f_{sa}, these frequencies are respectively 1.6 Hz and 0.6 Hz.

The resistance created by the throttle valve determines the behaviour of the system thing that can be easily seen in the graphs. As exposed before when the valve is closed or almost closed the system behaves as the air spring itself with nearly no volume flow through the valve, this cut off the auxiliary reservoir from the system and no energy is dissipated at the orifice which leads to the high amplification. When the valve is totally open or almost open the dissipation is low again. This happens because the volume flow is higher but with no pressure drop thing that lowers the damping in the system again and as result of that the amplification is also high but now at a lower frequency. Intermediate valve openings which give intermediate resistance to the flow of air show the best damping effect in the system and result in systems with better attenuation capabilities [24].

The best valve opening corresponds at the coincident point of all the possible openings, the point with the lowest amplification in our case is at f_B=0.8Hz. This corresponds with an opening of the valve that lets a space of 33.1832mm^2 or a pipe with an interior diameter of 6.5 mm. These optimum point is also described by Quaglia and Sorli using the ratio of natural frequencies Ω, their description also finds the coordinates of this point in a mathematical expression:

$$\Omega = \frac{f_s}{f_{sa}} \tag{5.8}$$

$$f_B = f_s \sqrt{\frac{2}{1+\Omega^2}} \qquad A_B = \frac{\Omega^2+1}{\Omega^2-1} \tag{5.9}$$

With:
- f_B natural frequency at the optimum point
- f_s natural frequency of the air spring alone
- f_{sa} natural frequency of the air spring with auxiliary reservoir
- Ω ratio of natural frequencies

Using this formulas it can be corroborated that the model is well done and the point of interference is the correct as the result of equation 5.9 gives f_B=0.8Hz as it does in the graph of figure 5.2, knowing this it can be determined using the other formula that the maximum amplification will be of 1.34dB at 0.8Hz.

This model doesn't perform well when applying vibrations with different amplitudes. Small amplitudes make the system behave more stiff since the auxiliary volume of air is not used, while larger amplitudes result in more flow through the throttle valve and a more flexible system [24].

For a better performance of the model in real simulation conditions a mathematical linearization has to be done. This could be done implementing Taylor series and considering the linearization point at the system at rest where x=0 and y=0, the air spring is at its design height and the pressure in the system $P_1 = P_2$ = m/A [24]. But in this case an experimental approximation was attempted using different methods and tests to find ξ and K parameters in the optimum opening valve position and also to the totally closed valve position (in order to compare results of the current solution installed and the solution studied). See annex B.2 for the test implementation.

Once the values are obtained and knowing that the system is a sub-damped system the parameters *b*, and *k* can be easily found using the equations 5.8, 5.9 and 5.10 knowing the mass, 1300Kg/4=325kg.

$$\omega_n = \sqrt{\frac{k}{m}} \tag{5.8}$$

With: m mass
k stiffness
ω_n natural frequency

$$\xi = \frac{b}{b_c} \tag{5.9}$$

With: ξ damping ratio
b damping
b_c critical damping

$$b_c = 2m\omega_n \tag{5.10}$$

For the case with the optimum valve opening, the parameters are *b*=509.6 Ns/m and *k*=208 N/m, for the totally closed valve the values are *b*=46.8 Ns/m and *k*=832 N/m.

Once the parameters are known a transfer function of the system can be designed knowing that the model is the shown at Figure 5.3.

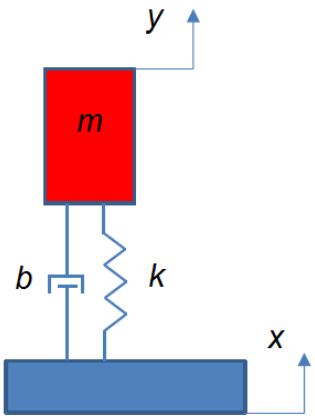

Figure 5.3 Model simplification of the system (*x* entrance displacement, *y* output displacement, *b* damping and *k* stiffness).

First the Lagrange equations of the model are find and combined:

$$m\ddot{y} = -b\,(\dot{y} - \dot{x}) - k\,(y - x) \tag{5.11}$$

After, the Laplace $\mathcal{L}$ transformation is made and manipulated until the desired transfer function is found:

$$ms^2Y(s) + bsY(s) + kY(s) = bsX(s) + KX(s)$$
$$Y(s)\,[ms2 + bs + k] = [bs + K]\,X(s) \tag{5.12}$$

$$H(s) = \frac{Y(s)}{X(s)} = \frac{bs + K}{ms^2 + bs + k} \tag{5.13}$$

With:

m	mass
k	stiffness
b	damping
K	gain

After the plot is done, the parameters *K* and *b* can be slightly changed as they are found with experimental methods, this parameters may change in order to adjust the lineal model to the nonlinear. To see if the linearization of the nonlinear model is good a comparison of the Bode plots is done, see Figure 5.4. If the plots coincide in a reasonable

way the linearization of the model will be considered appropriate and will be used further in the project for the next steps in the process.

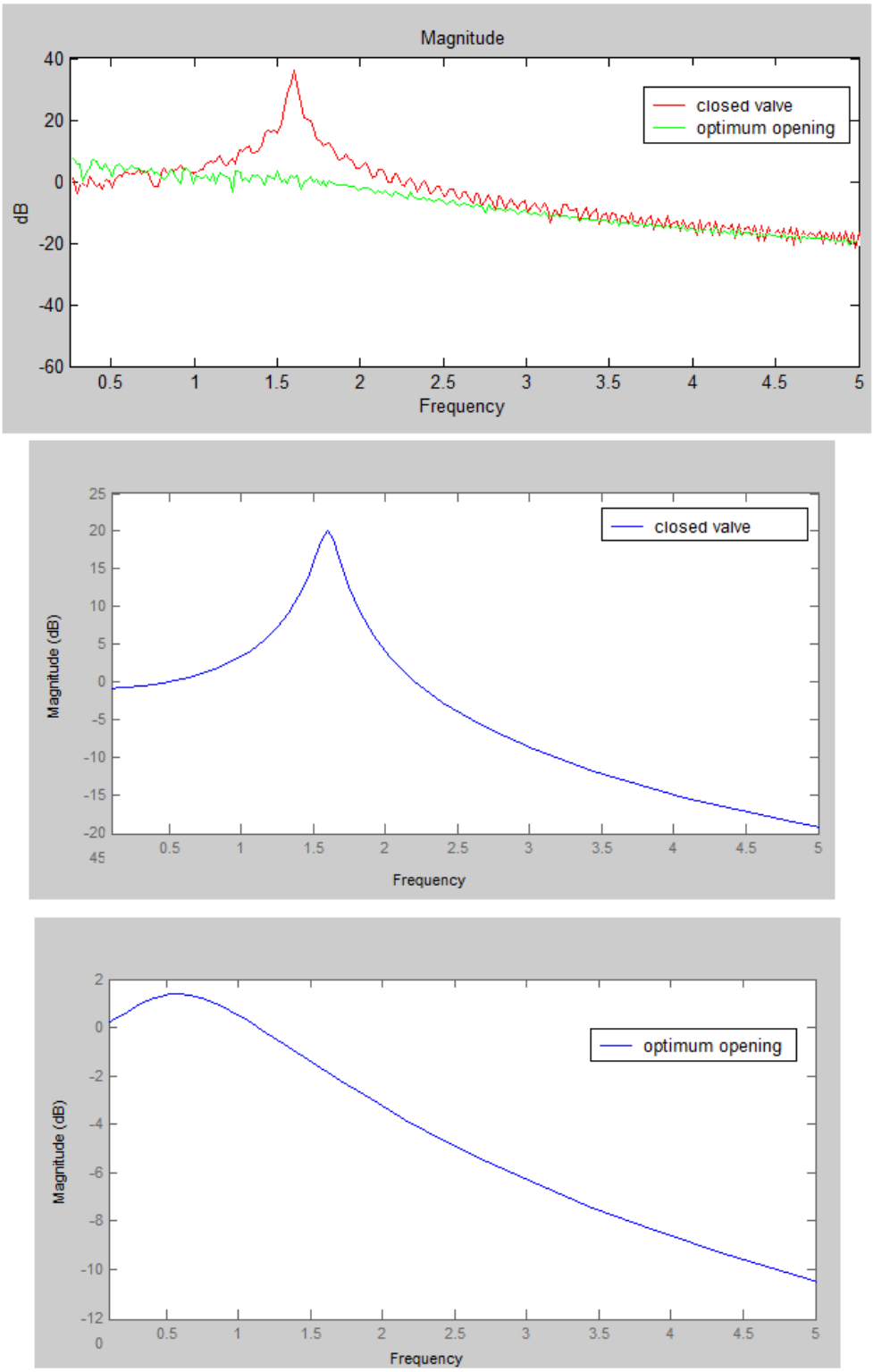

Figure 5.4 Bode plot comparison between the nonlinear model (on top) and the linear models.

Looking at the bode plots is easy to see that the linear model does not match the nonlinear in terms of magnitudes (dB). This can be explained as by using Tailor series when doing the linearization the result is a third order system and using the experimental approximation the result is a second order system which can not follow the real behaviour of the system.

Since the linearization of the model was not good enough a comparison of the response of the system with different valve openings will be shown using the original non lineal model. Figure 5.5 shows the response of a theoretical swept sine signal between 0.2 and 5Hz with an amplitude of 1,5cm of the opened valve, closed valve and optimum valve opening. This gives a good idea of the levels of attenuation obtained in the different cases and shows clearly that the good solution is the one with the optimum valve opening as it was seen before in figure 5.2.

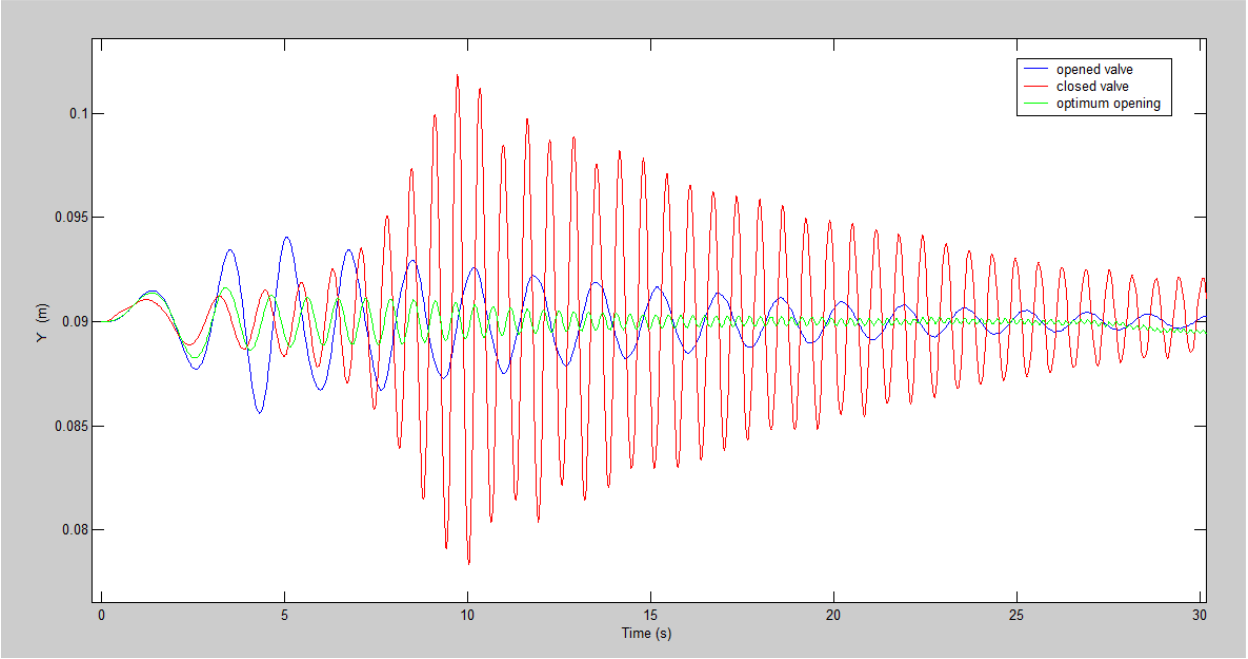

Figure 5.5 Behaviour of the system in response to an entrance of a theoretical swept sine signal between 0.2 and 5Hz with an amplitude of 1,5cm.

At Figure 5.5 the results are quite obvious and the confirmation that the system will behave better with the optimum valve opening is confirmed. Now the next step should be the extrapolation of this to the whole system.

5.3 Conclusions

In this chapter the modelization of an air spring Firestone Airstroke Airmount 131-M58-6155 [31] connected with an external reservoir of 37.5l using a throttle valve has been performed and tested. The first non lineal model obtained was attempted to be linearized but the results were not good enough. Even though consistent results could be delivered using the non linear model. The model with the auxiliary reservoir was probed to be better than the air spring alone. The model demonstrated that the position of the totally closed valve, which corresponds to the air spring alone, had high levels of amplification comparing it to the optimum valve opening using the auxiliary reservoir. The optimum valve opening found was of $3.31832 \cdot 10^{-5}$ m^2 equivalent to a pipe of 6.5mm of internal diameter. The best attenuation levels are reached using this configuration resulting in a natural frequency of 0.8Hz with a progressive attenuation that reach 20dB at 5Hz and 30dB at 10Hz with almost no amplification at lower frequencies.

After this positive results the possibilities of implementing the proposed solution are real. The next step of this process would be the modelling of the whole cabin in order to demonstrate, with even more elements, that the solution improves the actual situation.

Chapter 6

Conclusions and future perspectives

6.1 General conclusions

This project explained the problems that vibrations can do to the human body in order to demonstrate why this work was initiated. After that a list of the different suspension systems used to improve vibration isolation were presented and a first guess of which solution could be viable in the cabins was done.

After that an extensive evaluation of the low frequency vibration that affected the cabin cranes of Arcelor Mittal and its operators was delivered. Following the European directive [5] which sets on the minimum health and safety requirements regarding the exposure of workers to risks arising from physical agents (vibration) the project demonstrated that the actual suspensions are not good enough for the health of their operators even though the results obtained are legal just strictly using the Eurpoean directive [5].

This analysis also helped to understand the nature of the vibrations that affected the cabins and its results were used to study and develop a suspension system based on one of the elements discussed at the beginning of the project. The study performed in the cranes demonstrated that the implementation of an air spring with an auxiliary reservoir could be a good solution as no problems with natural frequencies between the vibration of the system and the proposed suspension where detected.

Finally a model of an air spring Firestone Airstroke Airmount 131-M58-6155 [31] connected with an external reservoir of 37.5l using a throttle valve has been performed and tested using Matlab Simulink. This was done in order to test if the proposed solution would improve the actual vibration levels. The results showed a big improvement of the situation comparing the results to the suspension installed in the first crane which consisted of four air springs with no auxiliary reservoir. After the good results obtained the first impression that installing the proposed solution could solve the vibration isolation problems seems evident.

6.2 Future work and perspectives

After the model of one air spring with the auxiliary reservoir the next step would be the model of this new suspension in a three dimensional setup. The linear model techniques to be used could be based on Harris' Shock and Vibration Handbook [35].

As a simplification to this model the centre of gravity could be considered to be symmetrical with respect to the suspension points as it can be seen at figure 5.3. The height of the centre of gravity could be considered to be at 2/3 of the total height of the crane.

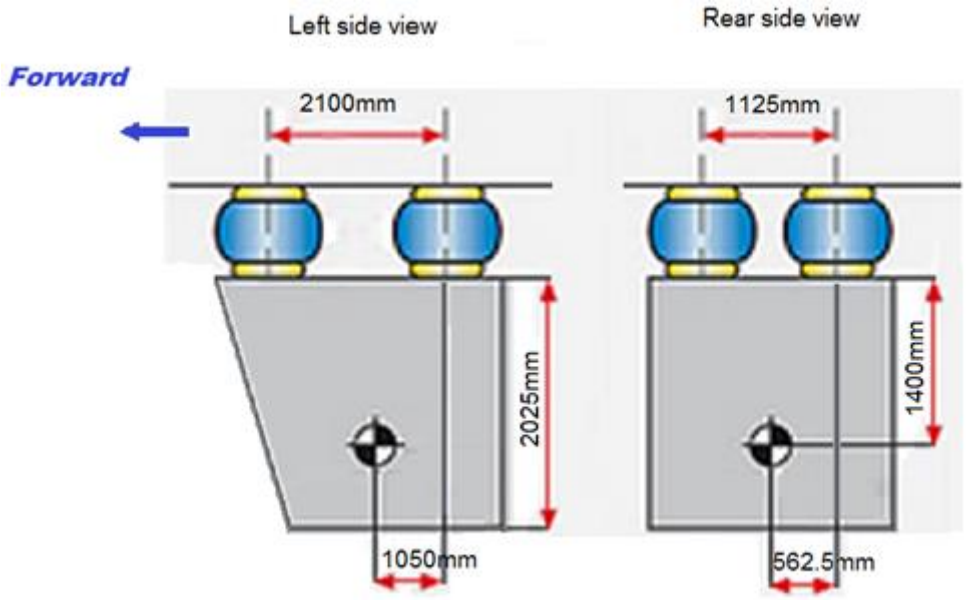

Figure 6.1 Sheme of the cabin with relative position of the center of gravity. (This is just a simplifyed drawing, the air suspensions are working always at compresion.)

After this new model and the interpretation of its results, which most certainly would be similar to the ones found in one air spring with his auxiliary reservoir, the solid proposal of trying the new suspensions in the cranes will appear. The last step should be the installation and testing of the new suspension to finally confirm the improved results obtained in terms of vibration isolation.

Acknowledgements

I would like to specially thank Dr. Koen Deprez for his expert advice and encouragement throughout this project, as well as his patience and always good attitude towards me. Without him this project would not have been possible.
I would also like to thank the company Arcelor Mittal and especially all the staff that collaborated during the testing days in the field.
Finally thank also the KU Leuven institution for borrowing all the material needed for the field tests.

Bibliography

[1] *ISO 2631-1, Mechanical vibration and shock – evaluation of human exposure to whole-body vibration –part 1: general requirements.* International Organization for Standarization, Geneva, 1997.

[2] Bernard. *Musculoskeletal Disorders and Workplace Factors A Critical Review of Epidemiologic Evidence for Work-Related Musculoskeletal Disorders of the Neck, Upper Extremity, and Low Back*. July 1997.

[3] Teschke K, Nicol A-M, Davies H. *Whole Body Vibration and Back Disorders Among Motor Vehicle Drivers and Heavy Equipment Operators A Review of the Scientific Evidence.* 1999.

[4] Waters T, Genaidy A, Viruet HB, Makola M. *The impact of operating heavy equipment vehicles on lower back disorders.* 2008.

[5] Council of the European communities, directive 2002/44/ec, on the minimum health and safety requirements regarding the exposure of workers to the risks arising from physical agents (vibration) (sixteenth individual directive within the meaning of article 16(1) of directive 98/391/eec). *Official Journal of the European Communities*, pages L177/13-19, 6 July 2002.

[6] *ISO 2631, Guide for the evaluation of human exposure to wholebody vibration.* International Organization for Standarization, Geneva, 1974.

[7] M.J.Griffin. *Handbook of Human Vibration*. 1990

[8] Von Gierke, Mccloskey & Albery. *Military performance in sustained acceleration and vibration environments.* 1991

[9] Sanders & McCormick. *Human factors in engineering and Design.*1993

[10] Aantaa, Virolainen, & Karskela. *Permanent effects of low frequency vibration on the vestibular system.* 1977

[11] Bovenzi & Hulshof. *An updated review of epidemiologic studies on the relationship between exposure to whole-body vibration and low back pain*. 1999

[12] Dupuis & Zerlett. *The Effects of whole-body vibration.* 1986

[13] Beevis & Foreshaw. *Back pain and discomfort resulting from exposure to vibration in tracked armoured Vehicles.* 1985

[14] Shwarze, Notbohm, Dupuis, & Hartung*, Dose-response relationships between whole-body vibration and lumbar disk disease- a field study on 388 drivers of different vehicles*.1998

[15] H. C. Boshuizen, P.M. Bongers, and C.T.J. Hulshof. *Self-reported back pain in tractor drivers exposed to whole-body vibration.* 1990

[16] M. Bovenzi and A. Zadini. *Self-reported low back symptoms in urban bus drivers exposed to whole-body vibration.* 1992

[17] Wasserman. *Human aspects of occupational vibration.* 1987

[18] Kittusamy & Buchholz. *Whole body vibration and postural stress among operators of construction equipment.* 2004

[19] Bonney. *Musculoskeletal disorders in health-related occupations* 1995

[20] Grandjean. *Fitting the task to the man.* 1988

[21] Mohr, Cole, Guild & von Gierke. *Effects of low frequency and infrasonic noise on man.* 1965

[22] Robyn Hopcroft and Michael Skinner. *C-130J Human Vibration*. 2005

[23] *BS6841 Measurement and evaluation of human exposure to whole-body mechanical vibration and repeated shock.* British Standards Institution, London*,* 1987

[24] Koen Deprez. *Assessment and improvement of the low-frequency vibrational comfort on agricultural machinery by optimized cabin suspension.* 2009

[25] Hendrickson USA, L.L.C. *http://www.hendrickson-intl.com/ProductInfo,* 2015

[26] Juratek ltd. *http://www.juratek.com/Airsprings.php, 2010*

[27] Y.Qiu and M. J. Griffin. *Transmission of fore-aft vibration to a car seat using field tests and laboratory simulation*, 264:135-155, 2003

[28] I. Hostens, K.Deprez, and H.Ramon. *An improved design of air suspension for seats of mobile agricultural machines.* 276:141-156, 2004

[29] BS6841, *Measurement and evaluation of human exposure to whole-ody mechanical vibration and repeated shock*. British Standards Institution, London, 1987

[30] The MathWorks Inc, *MATLAB help version 6.1.* Massachusetts, 2001

[31] Firestone Industrial Products, Inc. *Airstroke Actuators Airmount Isolators: Engineering Manual & Design Guide*, metric edition, Middlesex, England 1997.

[32] G.Quaglia and M. Sorli. *Air suspension dimensionless analysis and design procedure. Vehicle System Dynamics*, 35(6):443-475, 2001

[33] Zhongxing Li, Jiwei Guo, Mei Li, Xufeng Shen, Weijuan Jiang, Yue Wu. *Study on Damping of Air Spring with Additional Chamber*. Jiangsu university, China, 2011

[34] R.B.Bird, W.E. Stewart, and E. N. Lightfoot. *Transport phenomena.* John Wiley & Sons Inc., New York, 1960

[35] C.M. Harris. *Shock an Vibration Handbook.* Mc Graw-Hil Book Company, 3 edition, 1961

[36] LMS Engineering Services, *Vibro-aucoustic stdy on a prototype, phase 1.* Technical report, 1998

[37] Bauer, Wolfgang, Hydropneumatic Suspension Systems, 2011

[38] Carles Pous, Electronics and control, University of Girona, 2013

[39] V. Ramamurti1, S. Mithun, N. Prabhakar and T. Sukumar, *Experimental determination of damping ratios at higher modes for use in modal superposition*, India, 2012

Annex A

Matlab code for the vibration analysis

A.1 Matlab code for conditioning and filtering

A.1.1 Basic conditioning

The data obtained in the field had to be conditioned. The first step was to import the excel data to Matlab, changing the format of comas used in excel for the dots used in Matlab. This was done loading the whole file from the .xls to the program Notepad, there using the command Replace the comas where changed to dots. After the file was saved in .txt format, it had the structure that can be seen in figure A.1. The txt file was in all the tests 9 columns of data in which the 3 first columns where for the translations outside the cabin, the 3 next columns where used for calculating the rotations, and the last 3 for the translations inside the cabin.

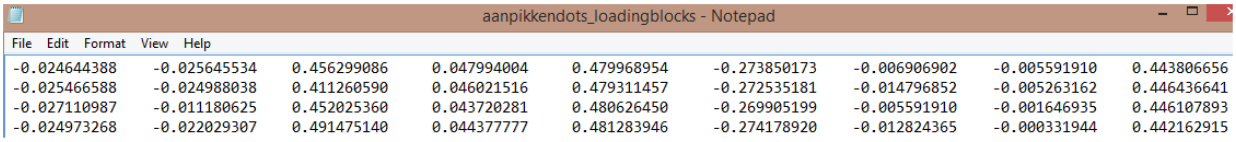

Figure A.1 Data format of the raw data.

For loading the data to Matlab and remove the average signal the code shown in figure A.2 was used in all the tests. All the m-files are created following the Matlab help [30].

```
load aanpikkendots_loadingblocks.txt
datafile=aanpikkendots_loadingblocks;
%O=outside the cabin,
%I=inside the cabin
%4, 5 and 6 are used for calculate the rotation
%Removal of the average signal
axooooO = datafile(:,1)-mean(datafile(:,1));
ayooooO = datafile(:,2)-mean(datafile(:,2));
azooooO = datafile(:,3)-mean(datafile(:,3));
ooooo4 = datafile(:,4)-mean(datafile(:,4));
ooooo5 = datafile(:,5)-mean(datafile(:,5));
ooooo6 = datafile(:,6)-mean(datafile(:,6));
axooooI = datafile(:,7)-mean(datafile(:,7));
ayooooI = datafile(:,8)-mean(datafile(:,8));
azooooI = datafile(:,9)-mean(datafile(:,9));
```

Figure A.2 Code for loading the data and remove the average signal.

After that a low pass filter with cut-off frequency of 50 Hz was used. See annex A.1.2. The next step was the resampling of the data from 20000Hz to 200Hz in order to accelerate the data processing of the computer and clean the signal. See figure A.3 for the code used. An evaluation of the correct resampling can be seen just checking the new length of the signal that in this case has to be the original one divided by 100.

```
%from 20000Hz to 200Hz sample time
fs=200
N = N0/100
%When we resample the data the time distribution it also has to change
t = linspace(0,63,N0/100);
%
[P,Q] = rat(fs/fs0);
abs(P/Q*fs0-fs);
axo0 = resample(axoo0,P,Q);
ayo0 = resample(ayoo0,P,Q);
azo0 = resample(azoo0,P,Q);
oo4 = resample(ooo4,P,Q);
oo5 = resample(ooo5,P,Q);
oo6 = resample(ooo6,P,Q);
axoI = resample(axooI,P,Q);
ayoI = resample(ayooI,P,Q);
azoI = resample(azooI,P,Q);
```

Figure A.3 Code for resampling the data.

The next step of the conditioning was the transformation of the values in volts to acceleration knowing that in our configuration 0.5 Volts equal to 9.81 m/s^2. Also we find the values for rotation using the equations (4.1) and (4.2) from the section 4.2.2. See figure A.4.

```
%Conversion from V to g. 0,5V=9.81m/s^2
%
ax0 = axo0.*(9.81/0.5);
ay0 = ayo0.*(9.81/0.5);
az0 = azo0.*(9.81/0.5);
o4 = oo4.*(9.81/0.5);
o5 = oo4.*(9.81/0.5);
o6 = oo4.*(9.81/0.5);
axI = axoI.*(9.81/0.5);
ayI = ayoI.*(9.81/0.5);
azI = azoI.*(9.81/0.5);
rx0=(ay0-o4)/0.24;
ry0=(o5-az0)/0.16;
rz0=(ay0-o6)/0.16;
```

Figure A.4 Code for finding rotation and the transformation of the data.

At this point the data was in the units that we needed for graphing the parameters in time domain, after plotting the accelerations the periods of time in which there was no signal were removed. Also some data needed changes in signal, because the orientation of the accelerometers inside and outside was not the same. See the code for plotting the acceleration in figure A.5. The code for the removed parts and change of signal in figure A.6 and finally the plots with the raw data and cut data in figure A.7.

```
%Acceleration plots axI ayI azI
%
figure
subplot(3,1,1);
plot(t,axI);
grid on;
set(gca,'fontsize',12,'fontweight','bold');
xlabel('Time (s)');
ylabel('A (m/s^2');
title('Acceleration axI,ayI,azI Plot');
xlim([0 max(t)]);
subplot(3,1,2);
plot(t,ayI);
grid on;
set(gca,'fontsize',12,'fontweight','bold');
xlabel('Time (s)');
ylabel('A (m/s^2');
xlim([0 max(t)]);
subplot(3,1,3);
plot(t,azI);
grid on;
set(gca,'fontsize',12,'fontweight','bold');
xlabel('Time (s)');
ylabel('A (m/s^2');
xlim([0 max(t)]);
```

Figure A.5 Code for plotting the acceleration data.

```
%20000Hz frequency rate we have 1440000 values 20000 per second
%so we have 72 seconds of data but we cut the signal at 63 seconds
%so we have 1260000 values
N0 = 1260000;
t0 = linspace(0,63,N0);
%
%After ploting the accelerations we are cutting the regions where there is no movement,
%we cut the signal at 63 seconds so we have 1260000 values now, also change the signal
%when necesary
%
axooo0 = axoooo0(1:1260000);
ayooo0 = ayoooo0(1:1260000);
azooo0 = azoooo0(1:1260000);
oooo4 = ooooo4(1:1260000);
oooo5 = ooooo5(1:1260000);
oooo6 = ooooo6(1:1260000);
axooo1 = axoooo1(1:1260000).*-1;
ayooo1 = ayoooo1(1:1260000).*-1;
azooo1 = azoooo1(1:1260000);
%
```

Figure A.6 The code used for cutting the signal.

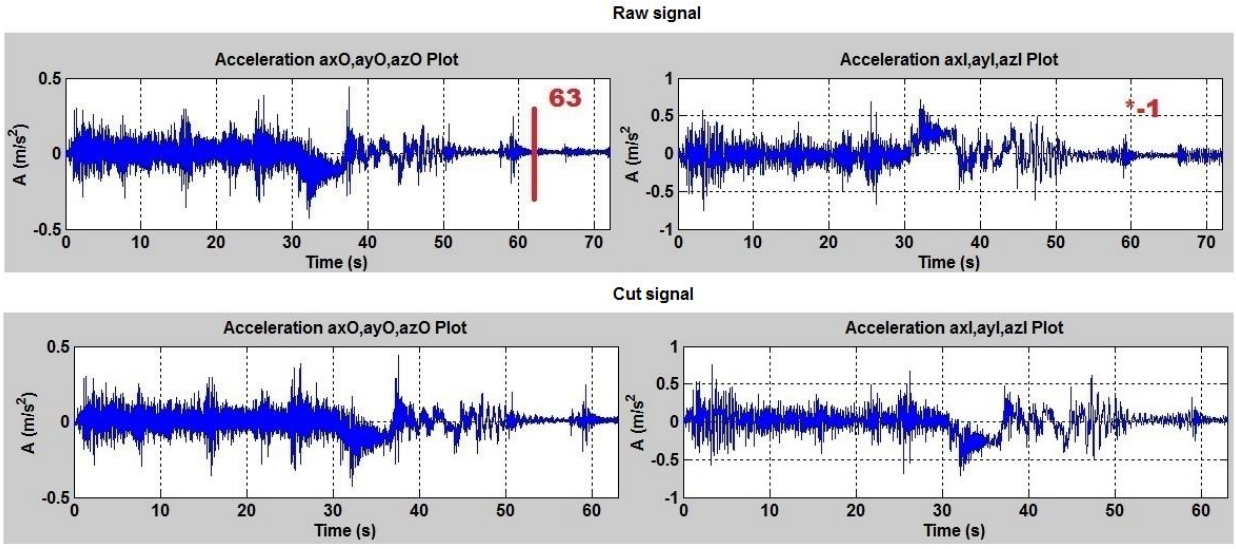

Figure A.7 Example of the procedure followed for cutting the signal. (Useful data until second 63 and acceleration inside multiplied by -1.)

The process explained here it's the one followed the first time that the data is looked at, after knowing where the signal has to be cut this last step can be moved just after the part where the average signal was removed in order to save time of computing.

All the code was find using the help command of Matlab that the program has incorporated.

A.1.2 Basic filtering

A low pass filter with cut-off frequency of 50 Hz was used, in this case a 5th order butter filter. The code used in Matlab [30] is showed in figure A.8.

```
fs0 = 20000;
fc = 50;
t0 = linspace(0,63,N0);
%
%Butter filter, 5 order, (2*frequency cut /frequency sample)
%
[B,A] = BUTTER(5,0.005);
axoo0 = filtfilt(B,A,axooo0);
ayoo0 = filtfilt(B,A,ayooo0);
azoo0 = filtfilt(B,A,azooo0);
ooo4 = filtfilt(B,A,oooo4);
ooo5 = filtfilt(B,A,oooo5);
ooo6 = filtfilt(B,A,oooo6);
axooI = filtfilt(B,A,axoooI);
ayooI = filtfilt(B,A,ayoooI);
azooI = filtfilt(B,A,azoooI);
```

Figure A.8 Code used for the low pass filter.

A plot for checking if the filter was properly done was also made with all the data samples, the code can be seen at figure A.9. And the plot for this evaluation can be seen at figure A.10. This code and plot was made based in the results of the magnitude spectrum showed in annex A.2.2.

```
%Trial plot for FFT ax0
%
AX01 = fft(axooo0);
AX01_mags = abs(AX01);
bin_vals = [0 : N-1];
fax_Hz = bin_vals*fs/N;
N_2 = ceil(N/2);
%
AX02 = fft(axoo0);
AX02_mags = abs(AX02);
bin_vals = [0 : N-1];
fax_Hz = bin_vals*fs/N;
N_2 = ceil(N/2);
%
figure
plot(fax_Hz(1:N_2),(AX01_mags(1:N_2)));
hold on;
plot(fax_Hz(1:N_2),(AX02_mags(1:N_2)),'r');
hold on;
legend('raw data','butter filtered data')
set(gca,'fontsize',12,'fontweight','bold');
xlabel('Frequency (Hz)');
ylabel('Magnitdue');
title('Magnitude spectrum ax0 ');
```

Figure A.9 Code used for the evaluation of good resampling and good filtering.

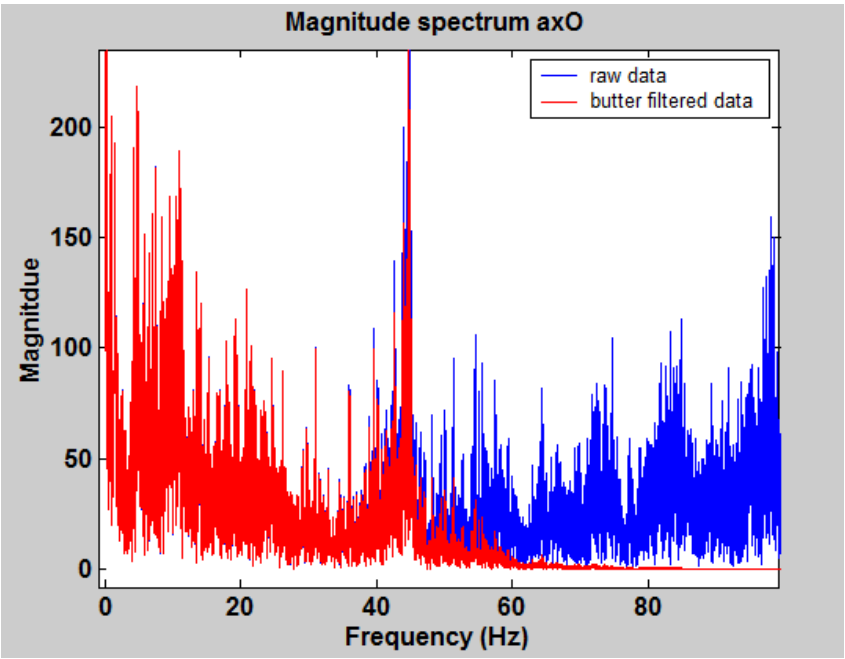

Figure A.10 Raw data and butter filtered data at 50Hz.

Looking at figure A.10 the good application of the filter it's easily seen as the frequencies bigger than 50-60Hz of the filtered data are attenuated significantly being it's magnitude almost 0.

A.2 Matlab code for the analysis of the data

A.2.1 Frequency domain analysis of the measurements

The first step for getting the magnitude spectrum is applying a Fast Fourier Transform FFT to the filtered data from the annex A.1.2, after the data is plotted. The values inside and outside the cabin are represented in the same graph to see the differences more easily. See the code for that application of the FFT and the plot at figure A.11. All the m-files are created following the Matlab help [30].

```
%
%Ploting FFT ax0 ay0 az0
%
AX0 = fft(ax0);
AX0_mags = abs(AX0);
AY0 = fft(ay0);
AY0_mags = abs(AY0);
AZ0 = fft(az0);
AZ0_mags = abs(AZ0);
bin_vals = [0 : N-1];
fax_Hz = bin_vals*fs/N;
N_2 = ceil(N/2);
%
% Plot at the same graph the magnitude spectrum inside and outside the cabin.
%
subplot(3,1,1);
plot(fax_Hz(1:N_2),(AX0_mags(1:N_2)));
hold on;
plot(fax_Hz(1:N_2),(AXI_mags(1:N_2)),'r');
grid on
legend('X Outside','X inside')
set(gca,'fontsize',12,'fontweight','bold');
title('Magnitude spectrum X Y Z in and outside')
xlabel('Frequency (Hz)')
ylabel('Magnitude')
%
```

Figure A.11 Code for plotting the magnitude spectrum.

The next step in a frequency domine analysis is the plot of the Power Spectral Density PSD. For doing so the Hanning window is applied and after that the PSD is done and plotted as before, showing the differences between inside and outside the cabin. See code for the PSD and plotting in figure A.12.

```
%Power spectrum plot ax0 ay0 az0
%
le = length(ax0);
nfft = 4096;
df = nfft*fix(le/nfft);
window = hanning(nfft);
nonverlap = nfft;
noverlap = nfft/2;
dflag = 'none';
[PSDWax0,f] = psd(ax0,nfft,fs,window,noverlap,dflag);
figure
subplot(3,1,1);
plot(f,10*log10(PSDWax0))
grid on
set(gca,'fontsize',12,'fontweight','bold');
title('PSD ax0 ay0 az0')
xlabel('Frequency (Hz)')
ylabel('Power/Frequency (dB/Hz)')
% Plot at the same graph the PSD inside and outside the cabin.
%
subplot(3,1,1);
plot(f,10*log10(PSDWax0));
hold on;
plot(f,10*log10(PSDWaxI),'r');
grid on
legend('X Outside','X inside')
set(gca,'fontsize',12,'fontweight','bold');
title('PSD X Y Z in and outside')
xlabel('Frequency (Hz)')
ylabel('Power/Frequency (dB/Hz)')
```

Figure A.12 Matlab code for the PSD application and plotting of the results.

After finishing the frequency domain analysis explanation and coding using Matlab the following step is the explanation of the code used for the time domain analysis.

A.2.2 Time domain analysis of the measurements

The first step for the time domain analysis is the filtering of the data using the weighting filters of the BS6841 [29]. At figure A.13 it is shown an example of how the data was filtered using Matlab [30].

```
ax0_in = ax0(1:length(ax0),:);
ay0_in = ay0(1:length(ay0),:);
az0_in = az0(1:length(az0),:);
o4_in = o4(1:length(o4),:);
o5_in = o5(1:length(o5),:);
o6_in = o6(1:length(o6),:);
axI_in = axI(1:length(axI),:);
ayI_in = ayI(1:length(ayI),:);
azI_in = azI(1:length(azI),:);
%
rx0_in=(ay0_in-o4_in)/0.24;
ry0_in=(o5_in-az0_in)/0.16;
rz0_in=(ay0_in-o6_in)/0.16;
T= (0:1/fs:(le-1)/fs)';
% x fil_inax filtering with BS 6841 used to quantify vibrations with respect to its effect on comfort and health
K=1;f4=2;f3=2;Q2=0.63;
fil_outax0=lsim([2*pi*K*f4^2  2*pi*K*f4^2*2*pi*f3],[f3  f3*2*pi*f4*f3/Q2  4*pi^2*f4^2*f3],ax0_in,T);
fil_outaxI=lsim([2*pi*K*f4^2  2*pi*K*f4^2*2*pi*f3],[f3  f3*2*pi*f4*f3/Q2  4*pi^2*f4^2*f3],axI_in,T);
%
% y fil_inay filtering with BS 6841 used to quantify vibrations with respect to its effect on comfort and health
K=1;f4=2;f3=2;Q2=0.63;
fil_outay0=lsim([2*pi*K*f4^2  2*pi*K*f4^2*2*pi*f3],[f3  f3*2*pi*f4*f3/Q2  4*pi^2*f4^2*f3],ay0_in,T);
fil_outayI=lsim([2*pi*K*f4^2  2*pi*K*f4^2*2*pi*f3],[f3  f3*2*pi*f4*f3/Q2  4*pi^2*f4^2*f3],ayI_in,T);
%
% z fil_inaz0 filtering with BS 6841 used to quantify vibrations with respect to its effect on comfort and health
f3=16; f4=16; f5=2.5; f6=4; Q2=0.55; Q3=0.9; Q4=0.95; K=0.4;
fil_outaz0=lsim([((2*pi*K*f4^2*f6^2)/(f3*f5^2)) ((2*pi*K*f4^2*f6^2)/(f3*f5^2))*(2*pi*(f3+f5/Q3)) ((2*pi*K*f4^2*f6^2)/(f3*f5^2))*(4*pi^2*(f3*f …
fil_outazI=lsim([((2*pi*K*f4^2*f6^2)/(f3*f5^2)) ((2*pi*K*f4^2*f6^2)/(f3*f5^2))*(2*pi*(f3+f5/Q3)) ((2*pi*K*f4^2*f6^2)/(f3*f5^2))*(4*pi^2*(f3*f …
%
% rotation fil_inrx, fil_inry, fil_inrz filtering with BS 6841 used to quantify vibrations with respect to its effect on comfort and health
K=1;f3=1;f4=1;Q2=0.63;
fil_outrx0=lsim([2*pi*K*f4^2  2*pi*K*f4^2*2*pi*f3],[f3  f3*2*pi*f4*f3/Q2  4*pi^2*f4^2*f3],rx0_in,T);
fil_outry0=lsim([2*pi*K*f4^2  2*pi*K*f4^2*2*pi*f3],[f3  f3*2*pi*f4*f3/Q2  4*pi^2*f4^2*f3],ry0_in,T);
fil_outrz0=lsim([2*pi*K*f4^2  2*pi*K*f4^2*2*pi*f3],[f3  f3*2*pi*f4*f3/Q2  4*pi^2*f4^2*f3],rz0_in,T);
```

Figure A.13 Matlab code for the weighting filter.

Once the data was filtered the values of RMS, crestfactor, VDV and VDV8h where calculated for each translation and rotation, an example of the Matlab code used for that is shown in figure A.14.

```
%RMS, Crest, VDV and VDV8h
%
%ax0, ay0, az0:
%
lenght=length(fil_outax0);
maxix0= max(fil_outax0);
RMS_x0 =(fil_outax0'*fil_outax0/lenght)^(1/2)
crestx0 = maxix0/RMS_x0
VDVx0 =(sum(fil_outax0.^4)/fs)^(1/4)
VDV_8h_x0 = (8*3600*(VDVx0^4)/(lenght/fs))^(1/4)
%
```

Figure A.14 Matlab code for the RMS, crestfactor, VDV and VDV8h.

Annex B

Matlab model design and linealization

B.1 Matlab Simulink code for the nonlinear model

The model is created using the equations explained in the section 5.2.1. The program Matlab Simulink was used to create the necessary blocks and connections as it can be seen at figure B.1. This model was initially created by Koen Deprez and was adapted to the new parameters required.

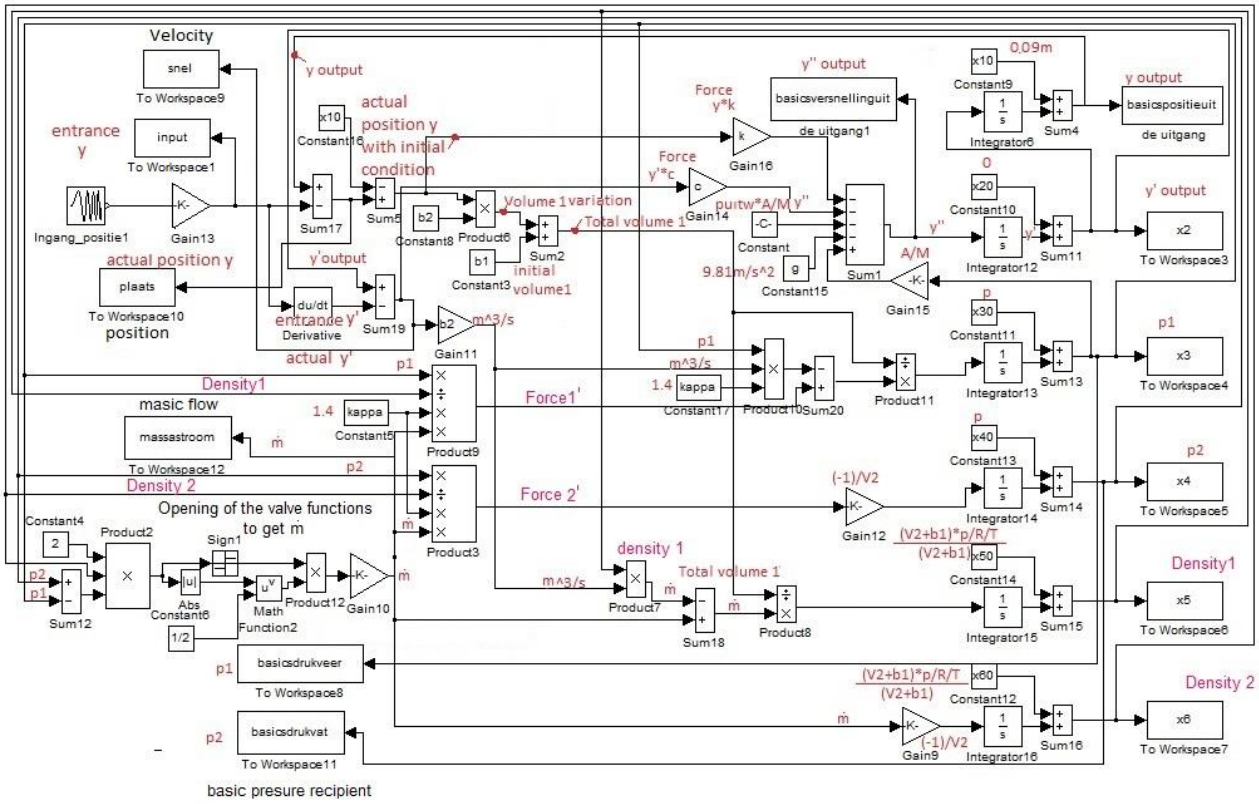

Figure B.1 Matlab Simulink code with some notes for a better understanding of the system.

Apart from this blocks it is needed a matlab code for the definition and understanding of the model. The matlab code used for determining the parameters is shown in figures B.2 and B.4, the values extracted from the manufacturer graph of the air spring [31] can be seen at figure B.3.

```
% The file gives the basic parameters for the simulation of the model of one airspring with
%auxiliar reservoir x6 times bigger than the original air spring volume.
% The airstroke airmount used is the type 131-M58-6155
% The cabine of the LK402 crane is of 1300Kg and we will use four airsprings with auxiliar reservoirs
%
% Wheight is Force/g
rustkracht=3188.25; % 1300*9.81=12753----> 12753/4=3188.25N
g=9.81;
M=rustkracht/g;     %kg
puitw=101325;       %Pa
% Looking at the tabe of the firestone catalog and knowing that each air spring has to hold 3188 N we use:
% The design height of 90mm
% Looking at the chart and enterning the force of 3188N our point fall between the 3 and 4 BAR curves, but
%closer to the 4 BAR.
% Which presure should we use?
% Effective Area = (Load at the presure)kN*100/Pressure(BAR)= 3575*100/4=893.75cm^2
% Now we cand find the required presure dividing the actual load by the effective area; 3188/893.75=3.56 BAR
% The initial volume can be easly found using: Volume = Effective area*height desing-0.02(for phisical
%constructive reasons)= 893.75cm^2*70mm= 6256.25cm^3
% The external reservoir has to be 6 times bigger than the original volme of the airspring so:
%0.00625625*6=0.0375375m^3
%
%
%A initial area of the air spring in m^2
A=0.089375;     %893.75cm^2  --->   0.089375m^2
kappa=1.4;
beginhoogte=0.09;   %m (initial height, design height)
b1=A*(beginhoogte-0.02); %b1=A*(initial height-0.02);   %m^3 initial volume
b2=0.012;   % m ^ 3 / m slope of increase in volume as a function of the height taken from the graph:
%(1000cm^3-400cm^3/100mm-50mmm=600cm^3/50mm=0.0006m^3/0.05m=0.012m^3/m
V2=0.0375 % the volume of the external reservoir in m^3 = initial volume with the -0.02 consideration*6
%(calculated before)
S=0.0000331832 %(this value is just an example, is the value to choose the opening of the valve m^2)
```

Figure B.2 Basic parameters for the model using the manufacturer catalogue.

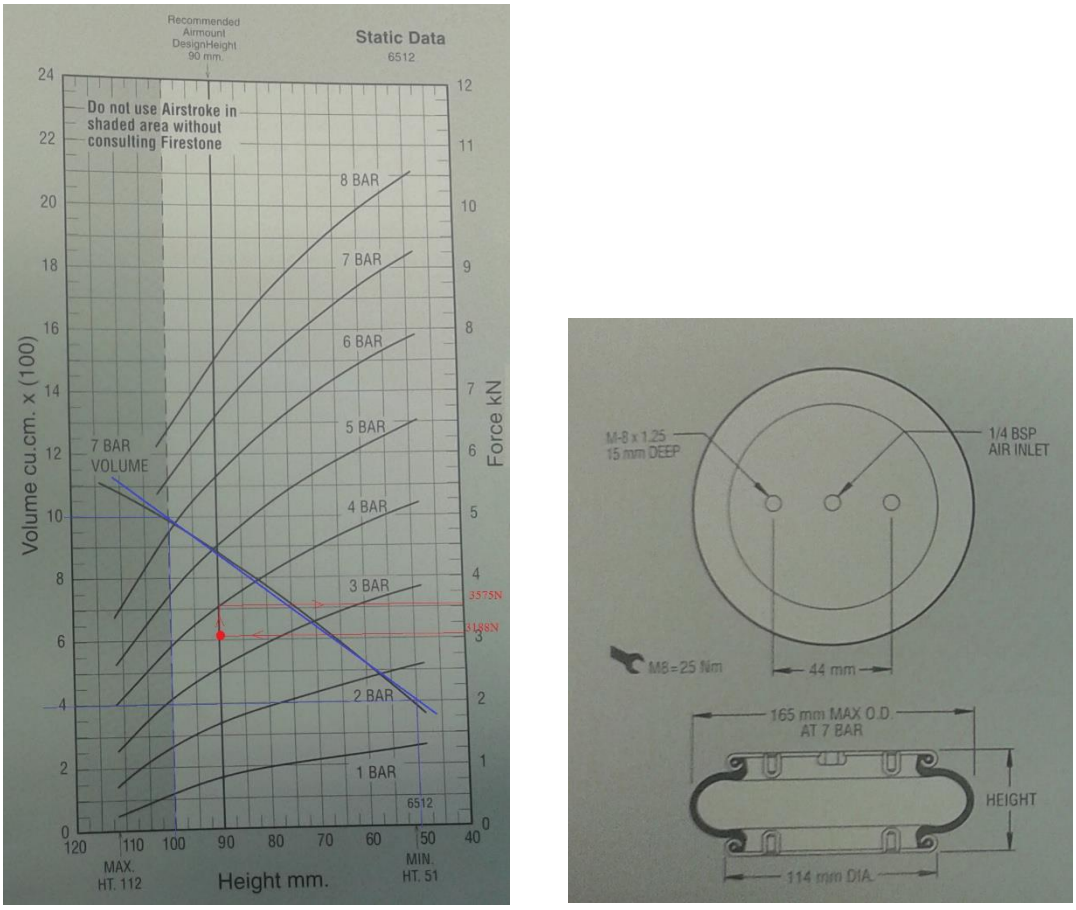

Figure B.3 Graph with the behaviour of the air spring in the left and physical dimensions in the right [31].

```
pstart=rustkracht/A; %Presure at the start
p=puitw+pstart;      %Presure
% mass in function of the volume and the presure
R=288;      %Constant R
T=293;      %Temperature
%
massa=(V2+b1)*p/R/T;
%
ro=massa/(V2+b1);%density
%
x10=beginhoogte;%initial height
x20=0;
x30=p;%presure
x40=p;
x50=ro;%density
x60=ro;
```

Figure B.4 Last constants and other parameters for the model.

After running the model the only thing that is needed, apart from plotting the inputs, outputs, pressures and densities for seeing the behaviour of the model, is the plotting of the transfer function of the system. To do so we can not use the command bode plot as we do not have a transfer function, to get the plots the code of figure B.5 is used.

```
%%FFT method for finding Transfer Function
%
% FFT of input data
Input = fft(input);
% FFT of output data
Output = fft(basicspositieuit);
fft_ratio = Output ./ Input;
subplot(2,1,1)
%Magnitude
y=20*log10(abs(fft_ratio));
x=(0:80/4096:(80-(80/4096)));
plot(x,y,'k');
legend('opened valve','closed valve','optimum opening','other openings')
xlim([0.25 5])
hold on
title('Magnitude');
xlabel('Frequency');
ylabel('dB');
subplot(2,1,2)
%Phase
semilogx((180/pi)*angle(fft_ratio))
mag = 20*log10(abs(fft_ratio));
phase = (180/pi)*angle(fft_ratio);
x2=(0:80/4096:(80-(80/4096)));
plot(x2,phase,'k')
legend('opened valve','closed valve','optimum opening','other openings')
xlim([0.25 5])
hold on
title('Phase');
xlabel('Frequency');
ylabel('°Phase');
%%Position plot
figure
plot(x,input);
hold on
plot (x, basicspositieuit);
```

Figure B.5 Code for the transfer functions of the model with different valve openings.

The plots of position, pressure, and densities are simply the values plotted against time, as it shown at the end of the code of figure B.5.

B.2 Linearization of the nonlinear model

It is necessary to find the parameters ξ and K for the linearization of the system. Different experimental tests can be performed in order to do so. The easiest way to obtain these parameters is introducing an input step to the nonlinear model and see how the system responds to it, this methodology is called bump test. In figure B.6 an example of how to analyse the test with the necessary equations is shown. The test is based on time to reach different specific points in the time-position response graph of the system, using this timings and positions it is possible to find ξ and K.

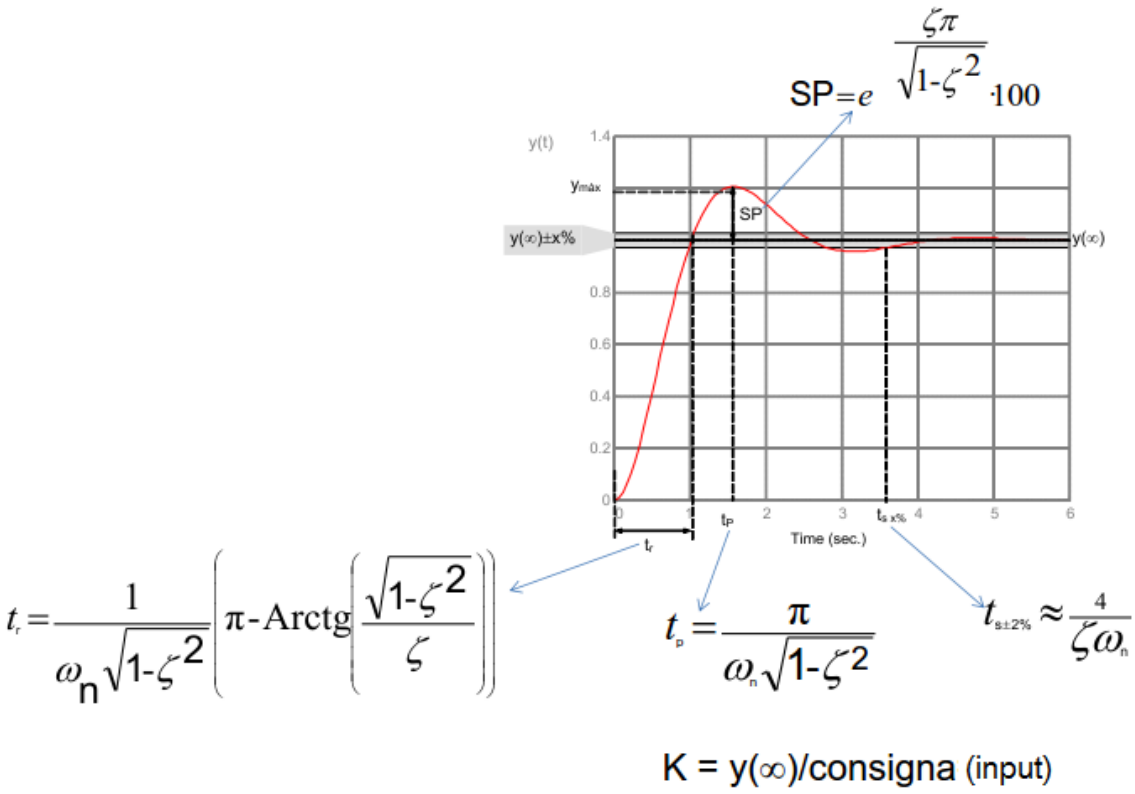

Figure B.6 Interpretation of a bump test with the necessary equations [38].

This test was performed with the totally closed valve and optimum valve opening. The bump test results were useful for the calculation of the K but not the ξ as in the case of totally closed valve the equations were giving a ξ of almost 1 and the graphical interpretation clearly illustrated that the value should be lower than 0.2 al least, see figure B.7. The K obtained in the two tests was almost the same with a value of K=0.94.

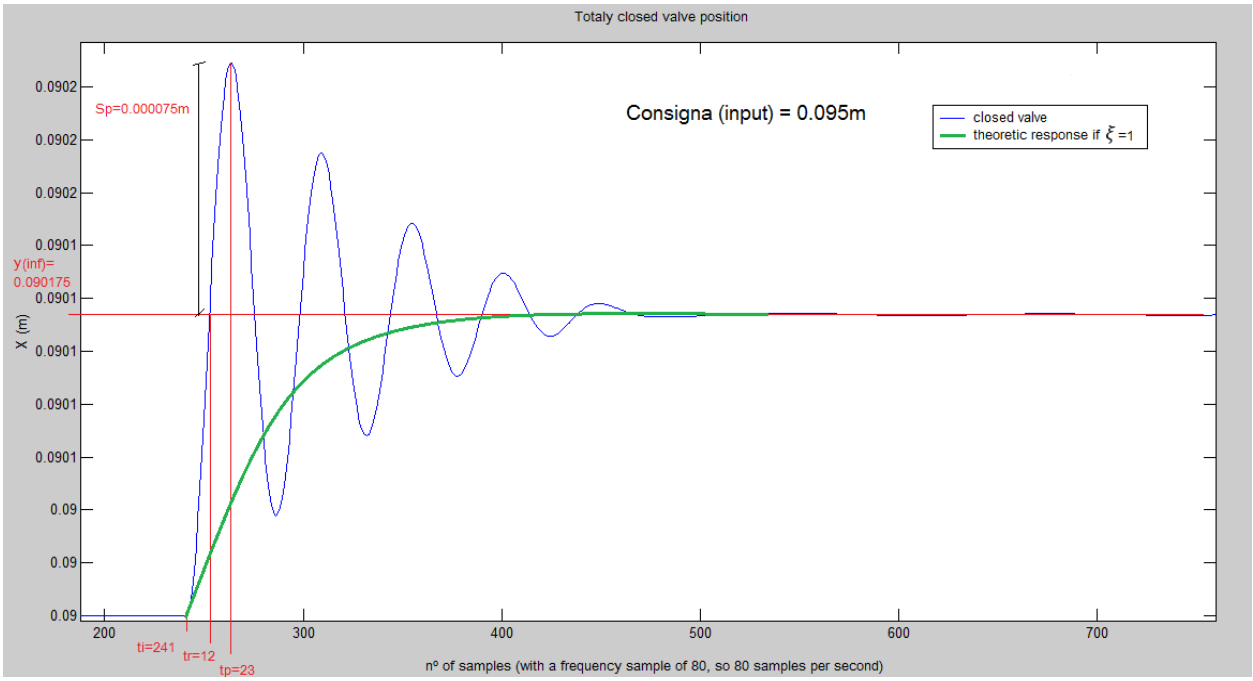

Figure B.7 Results of the bump test with the totally closed valve and a theoretical curve of $\xi = 1$.

The other test performed in order to find ξ was the $\sqrt{2}$ method [39]. This method consists in analysing the bode magnitude plot of the system and then apply a simple rule as it is shown in figure B.8.

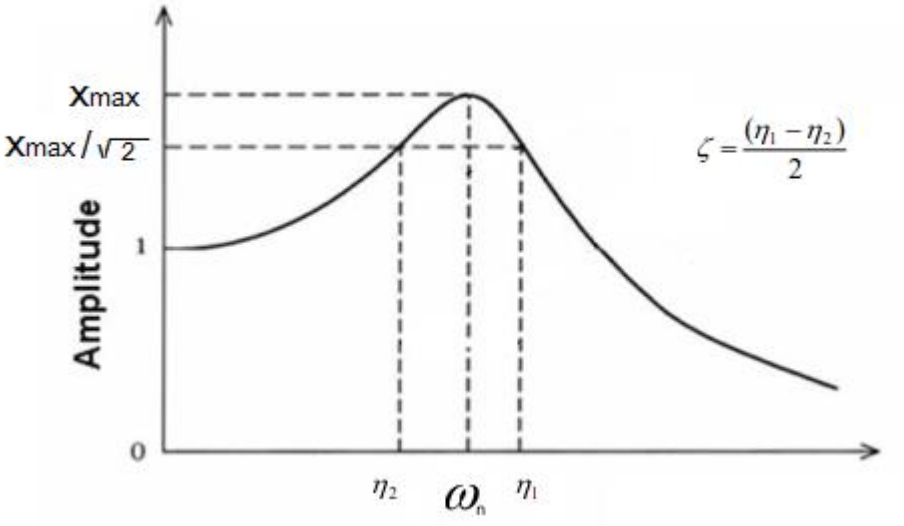

Figure B.8 Explanation of the $\sqrt{2}$ method [39].

In figure B.9 the result of the $\sqrt{2}$ method for the totally closed valve is shown. Being as result ξ=0.045.

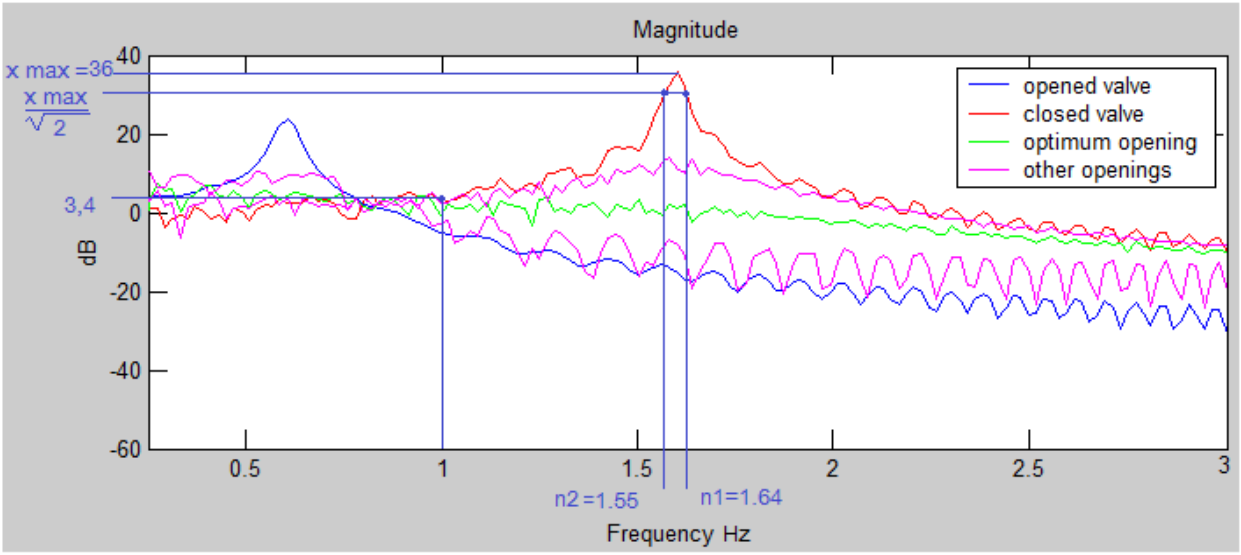

Figure B.9 Result of the $\sqrt{2}$ method for the totally closed valve.

For the optimum valve opening it is easy to see that the error of the result is going to be high using this method but it can also be seen that this position corresponds to the one with the lowest amplification and this is always related to a ξ =1, see figure 4.13.
So in our model ξ will be considered of 0.98 which could give a good approximation of the nonlinear model.

Finally once the transfer function is designed, as explained in chapter 5.2, the plots of the linearization models are obtained using the code showed at figure B.10, the value of the gain has been changed until matching the 0 at the beginning of the plot.

```
%TESTING
%
%optimum valve opening
figure
num = [494 210];
den = [325 494 208];
sys = tf(num,den)
bode(tf(num,den));
%closed valve
figure
num = [46.8 750];
den = [325 46.8 832];
sys = tf(num,den)
bode(tf(num,den));
```

Figure B.10 Matlab code for the linearization of the models.

Annex C

AIB-VINÇOTTE International test

The company AIB-VINÇOTTE International made their measurements just considering the values of effRMS and VDV but no VDV8h were shown in their tests as they are not mandatory in the ISO 2631-1 [1]. Their tests were performed in the seat where the operator works, see figure C.1. The results that they gave were okay but looking at the VDV8h of their measures, see table C.1, it can be seen that the values are quite high, equation (4.5) from section 4.3.4 for the calculation of VDV 8h, (remembering that the maximum value for VDV8h is 9.1 m/s1.75).

Figure C.1 Disposition of the measuring device used by the company.

Measurement	**VDV8h X** ($m/s^{1.75}$)	**VDV8h Y** ($m/s^{1.75}$)	**VDV 8h Z** ($m/s^{1.75}$)
72 LK 403	4.23	(3.95)	5.25
73 LK 403	4.50	(3.85)	6.28
74 LK 403	4.17	(3.26)	4.86
76 LK 402	(3.82)	(3.76)	6.81
77 LK 402	4.30	(3.96)	6.79
78 LK 402	4.06	4.02	7.31

*The values in parenthesis are for tests with crest factors under 7 m/s^2.

Table C.1 Values of the VDV8h for the tests performed by AIB-VINÇOTTE International.

The values in the table C.1 show that the comfort situation, especially in Z translation is quite bad for the operators, the ISO norm [1] doesn't contemplate the VDV8h as a critical factor but Griffin does [7] and in our project we consider it important as well.

In figure C.2 and C.3 the tests results given by AIB-VINÇOTTE International in the two cranes can be seen.

Measurements according to ISO 2631-1: 1997

Company: Arcelor Mittal Gent - Equipment: Loopkraan LK 403

Measurement conditions

1	Bestuurder Van Cronenburg Marc
2	Gewicht 96 Kg
3	Vervoer van coils
4	Aanpassingen aan de structuur van de stuurcabine (bedoeling: vermindering van de trillingsamplitudes)

Timing			Measurements					Evaluation	
Measurement	Date	Duration	X_RMS (m/s² rms)	X_maxiMTVV)	X_C.F.	X_VDV	X_Peak (m/s² rms)	Limit (B.2) (min)	VDV/$a_w T^{1/4}$
72	28/01/2014	0:10:01	0.1826	0.8203	9.555	1.608	1.7448	1440	1.50
73	28/01/2014	0:10:01	0.1811	0.8731	8.702	1.711	1.576	1440	1.61
74	28/01/2014	0:09:54	0.1643	0.8999	8.752	1.583	1.4379	1440	1.64
Measurement	Date		Y_RMS (m/s² rms)	Y_maxiMTVV)	Y_C.F.	Y_VDV	Y_Peak (m/s² rms)	Limit (B.2) (min)	VDV/$a_w T^{1/4}$
72	28/01/2014	0:10:01	0.193	0.7445	5.575	1.503	1.076	1440	1.32
73	28/01/2014	0:10:01	0.178	0.6038	6.49	1.466	1.1552	1440	1.40
74	28/01/2014	0:09:54	0.1454	0.5189	5.854	1.239	0.8512	1440	1.45
Measurement	Date		Z_RMS (m/s² rms)	Z_maxiMTVV)	Z_C.F.	Z_VDV	Z_Peak (m/s² rms)	Limit (B.2) (min)	VDV/$a_w T^{1/4}$
72	28/01/2014	0:10:01	0.2166	0.801	8.042	1.998	1.7419	1440	1.57
73	28/01/2014	0:10:01	0.2436	1.201	10.12	2.387	2.4657	1440	1.67
74	28/01/2014	0:09:54	0.1795	0.744	9.479	1.842	1.7014	1440	1.74

Legend :

XXX: Exposure time lower than 4 hours

Maximum value

XXX : Exposure time between 4 and 8 hours

XXX VDV larger than 1.75

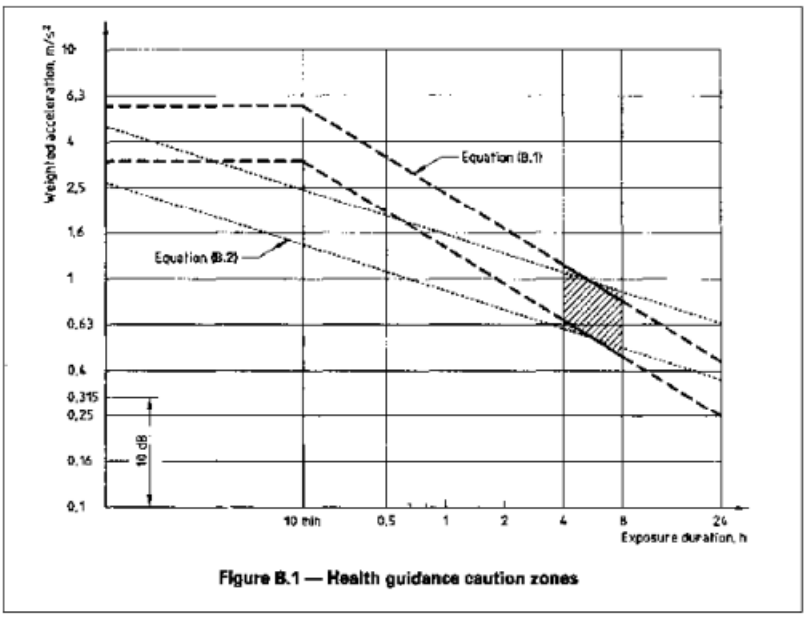

Figure B.1 — Health guidance caution zones

Figure C.2 Measurement of the crane LK403.

Measurements according to ISO 2631-1: 1997

Company/ ARCELOR Mittal Gent - Equipment:Loopkraan LK402

Measurement conditions	
1	Bestuurder: Van Cronenburg Marc
2	Gewicht: 96 Kg
3	Vervoer van coils
4	GeEn aanpassingen op de kraan

Timing			Measurements					Evaluation	
Measurement	Date	Duration	X_RMS (m/s² rms)	X_maxiMTVV)	X_C.F.	X_VDV	X_Peak (m/s² rms)	Limit (B.2) (min)	VDV/$a_w T^{1/4}$
76	28/01/2014	0:10:03	0.1881	0.5681	5.921	1.454	1.1137	1440	1.31
77	28/01/2014	0:10:03	0.1891	0.8497	14.88	1.636	2.8132	1440	1.47
78	28/01/2014	0:09:02	0.1908	0.7976	11.12	1.504	2.1222	1440	1.34
Measurement	Date		Y_RMS (m/s² rms)	Y_maxiMTVV)	Y_C.F.	Y_VDV	Y_Peak (m/s² rms)	Limit (B.2) (min)	VDV/$a_w T^{1/4}$
76	28/01/2014	0:10:03	0.1819	0.5421	6.107	1.431	1.1108	1440	1.34
77	28/01/2014	0:10:03	0.1857	0.6497	6.127	1.508	1.1378	1440	1.38
78	28/01/2014	0:09:02	0.1874	0.7083	7.138	1.489	1.3376	1440	1.35
Measurement	Date		Z_RMS (m/s² rms)	Z_maxiMTVV)	Z_C.F.	Z_VDV	Z_Peak (m/s² rms)	Limit (B.2) (min)	VDV/$a_w T^{1/4}$
76	28/01/2014	0:10:03	0.2813	1.2256	8.638	2.592	2.43	1440	1.57
77	28/01/2014	0:10:03	0.2678	1.3467	9.514	2.585	2.5478	1440	1.64
78	28/01/2014	0:09:02	0.2711	1.5696	12.16	2.709	3.2976	1440	1.70

Legend :

XXX: Exposure time lower than 4 hours

Maximum value

XXX : Exposure time between 4 and 8 hours

XXX VDV larger than 1.75

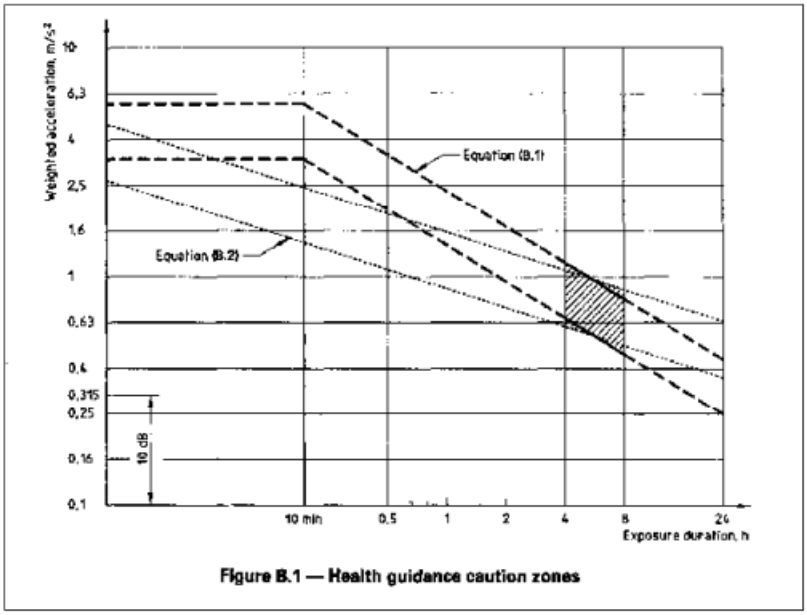

Figure B.1 — Health guidance caution zones

Figure C.3 Measurement of the crane LK402.